R. & M. No. 2792
(12,711, 12,308)
A.R.C. Technical Report

MINISTRY OF SUPPLY

AERONAUTICAL RESEARCH COUNCIL
REPORTS AND MEMORANDA

An Experimental Study of Three-dimensional High-Speed Air Conditions in a Cascade of Axial-flow Compressor Blades

By

K. W. Todd, M.Eng.,
of Metropolitan-Vickers Electrical Company, Ltd.

LONDON : HER MAJESTY'S STATIONERY OFFICE
1954
TEN SHILLINGS NET

An Experimental Study of Three-dimensional High-Speed Air Conditions in a Cascade of Axial-flow Compressor Blades

By

K. W. Todd, M.Eng.

of Metropolitan-Vickers Electrical Company, Ltd.

Communicated by the Principal Director of Scientific Research (Air), Ministry of Supply

*Reports and Memoranda No. 2792**

October, 1949

Summary.—Detailed investigations have been made by optical and physical methods in a high-speed wind tunnel of the flow characteristics of two compressor blade cascades.

In Part 1 a representative high-camber cascade was examined at zero incidence over entry air velocities ranging from low to critical. Traverses were made of discharge angles and wake losses at all heights so that a relation between two and three-dimensional losses could be obtained. Some records were also made of the nature of the vortices induced in the discharge flow.

In Part 2 the blade and passage design was conditioned by the findings of Part 1, with the aim of so modifying the cascade that its efficiency in the critical flow region would be improved. Optical and physical examinations were again carried out over a range of both incidence and velocity.

The results from Part 1 indicate that although fully developed shock formations can be used to bring about reduction in profile drag, the net performance of a conventional cascade is prohibitively low when shock occurs, by reason of the shock losses themselves.

The results from Part 2 show that by delaying the advent of shock, and by reducing its intensity and complexity, an improvement in high-speed performance can be achieved, although at a somewhat limited incidence range.

Introduction.—Tests on a turbine runner blade cascade, published elsewhere by Todd[1] (1947) have revealed that certain peculiarities of the shock-wave development result in improvement of the cascade efficiency at conditions of critical entry velocity.

It was therefore decided to conduct an analogous series of tests into flow conditions through a cascade of compressor blades of conventional section, high camber and medium stagger (Part 1).

As a result of these tests it was shown that at the design incidence the conventional cascade shock stalled at some 75 per cent of the critical inlet velocity. Optical analysis of this shock stall led to the conclusion that its initiation was accelerated by the rapid curvatures incurred at and near to the blunt leading edge, and that a contributory factor was also the existence of the position of maximum thickness of the blade at 32·6 per cent of the chord.

Moreover, the conventional section, when set up at medium pitch and stagger, yielded a passage shape in which the ratio of inlet area to throat area (contraction ratio) was less than unity, and whence the tendency to achieve local sonic velocity ahead of the geometrical throat position was incipient.

*Received 16th February, 1950.

It was decided therefore in Part 2 to construct a cascade in which the blade section had no rapid curvatures near the leading edge, *i.e.*, in which the nose was razor sharp, and in which the point of maximum thickness was at 50 per cent chord. The passages were constructed to the same pitch and stagger as in Part 1 but the experimental blade camber was reduced so that contraction ratio of unity was achieved at zero incidence.

Apparatus.—The Metropolitan-Vickers high-speed cascade tunnel, described elsewhere by Todd[1] (1947) was used throughout these investigations. This is a suction tunnel with a working-section of 10 sq in. having boundary-layer extraction through slots provided on all four walls, the quantity extracted from each slot being independently controlled. The tunnel motive power is a supercharger used as a suction pump and driven through increasing gear from a 400 h.p. variable speed a.c. motor.

Instrumentation.—The majority of the tests were made with a cylindrical pitot-yawmeter of 0·070 in. o.d. having 0·010 in. pitot and yaw holes, with the angle included between the radial axes of the yaw holes at 100 deg. The instrument projected through the tunnel floor and roof, lying in the plane of the blades, so that resistance to flow was constant irrespective of the height at which observations were made, or of the angular setting.

All static pressures were observed by 0·020 in. wall tappings, the holes being slightly chamfered to eliminate burrs.

Investigations of secondary flow in Part 1 involved searches for trailing-edge vortices downstream of the cascade. This necessitated the manufacture and development of a special instrument in the form of an air-floated swirl vane with remote observation of direction and speed of rotation.

Optical testing was done by the Toepler schlieren system, using high-quality parabolic mirrors of 36 in. focal length, and 6 in. diameter. As source of light either a continuous mercury-arc lamp or a short-duration Xenon-filled flash-lamp was used, giving exposure times of the order of 3 microseconds. When optical studies were in progress the brass tunnel roof and floor were replaced by glass panels, the blades being pinned into position by pegs let into holes drilled in the glass.

All these specially developed instruments, together with their calibrations, are described elsewhere by Todd[2] (1949).

Cascade Details (*see* Fig. 1):—

	Part 1	*Part* 2
Section	RAF 27 + 10 per cent	8068 G
Camber	45 deg	27·5 deg
Chord	1·0 in.	0·926 in.
Stagger	— 30 deg	— 30 deg
Height	2·0 in.	2·0 in.
Blade inlet angle	37·5 deg	47·5 deg to line of cascade
Blade outlet angle	97·5 deg	105 deg to line of cascade
Pitch/chord ratio	0·80	0·865
Aspect ratio	2·0	2·16
Number of blades	8	8
Maximum-thickness/chord	0·1104	0·081
Contraction ratio at 0 deg incidence	0·915	1·02

In Part 1 choice of camber, stagger, and aspect ratio was made specifically to create the full gamut of shock and secondary-flow conditions within the scope of the tunnel, and within a passage which would be large enough for satisfactory optical investigation. It was appreciated that the low aspect ratio might involve poor absolute performance of the blading, but as the objectives were qualitative rather than quantitative, this limitation was accepted.

Inlet Conditions.—In Fig. 2 is shown a model of the arrangement of apparatus and measuring points about the test cascade. It will be noted that two rows of upstream static-pressure tappings were provided, with the floor and roof boundary-layer suction-slots disposed between them. The side-wall suction-slots were formed between the extremities of the inlet side walls and the end blade leading edges.

Side-wall suction quantities were manipulated until the static pressures between points B and C in the second static row were as uniform as possible for the inlet Mach Number required. The floor and roof-suction quantities were then adjusted in parallel until the static pressure at A in the first static row equalled the mean of the pressures between B and C.

It was thus ensured that a column of air in which the streamlines were reasonably parallel in height and width was presented to the central portion of the test cascade. The floor and roof boundary layers were by no means removed by this technique since only some 3 per cent of the mass flow was extracted, but they were reduced from a thickness of 15 per cent of blade height to 10 per cent of its height, when measured immediately ahead of the blades.

A typical example of entry conditions is plotted in Fig. 3.

Outlet Conditions.—No outlet side walls were applied in these tests, although the effect of their presence upon discharge conditions was known to be considerable. The qualitative nature of the programme, and the simplification thus ensured, justified their exclusion. The floor and roof of the tunnel working-section was, of course, continued well downstream of the cascade.

All traverses were made in a plane one-chord downstream of the cascade trailing edges. They were arranged to span two adjacent pitches, from the middle of the passage bounded by blades 3 and 4, to the middle of that between blades 5 and 6. Observations were taken at intervals of 0·1 in. over the span of 1·8 in., giving 17 readings per traverse.

In addition to the standard 'mid-height' traverses for providing two-dimensional characteristics, Part 1 of the programme included a series of 10 traverses at heights varying from 0·1 in. from the floor to 1·9 in. from the floor for the purpose of assessing three-dimensional characteristics.

Downstream static pressures were observed by roof tappings arranged at intervals of 0·2 in. across the same two-pitch span as for the pitot-yaw traverses. Results were generally found to be uniform across this range, and mean values only have been recorded. It should be realised however that when shock conditions are present in a flow the wall-tapping statics do not necessarily represent the local midstream pressures.

Test Programme. Part 1.—The cascade was tested at zero incidence only. It was first calibrated in terms of inlet velocity by running at a full range of supercharger impeller speeds, the boundary-layer suction quantities being adjusted at each speed to give the optimum inlet static-pressure uniformity. Inlet static, pitot, and yaw values were then noted so that Mach number, Reynolds number and actual incidence could be plotted against supercharger impeller speed.

Impeller speed rather than inlet Mach number was chosen as abscissa for all plots so that clustering of the results where the inlet Mach number was approaching its critical (maximum) value might be avoided.

Inlet conditions having been ascertained, the cascade was placed between glass panels for the recording of a complete set of schlieren photographs at Mach numbers up to and well within the critical flow region.

Optical study was followed by detailed downstream traversing of the pitot-yawmeter and static-pressure observations at mid-height of passage.

The complete two-dimensional characteristics resulting from these tests were oriented to the shock records and used for selection of five representative speeds at which to carry out three-dimensional investigations. At these five points, non-mid-height pitot-yaw, and swirl-vane studies were completed, after which the whole programme was reviewed and analysis and conclusions leading to Part 2 were evolved.

The method of calculation of performances is shown in the Appendix.

Part 2.—The range of incidence selected was from — 10 deg through 5 deg intervals to + 10 deg with particular attention to the zero incidence setting. At each incidence a full range of inlet velocities was examined.

As in Part 1 the cascade was first calibrated in terms of inlet velocity, then studied by schlieren technique, then examined by traversing of instruments, and finally checked for outlet static pressure values.

In Part 2 testing was confined to mid-passage height, and use was not made of the swirl vane.

Test Data. Part 1.—*Optical Tests.*—In Fig. 4 are shown six sets of schlieren photographs of the development of shock and wake formation from the point at which compressibility first becomes evident up to the extreme suction condition available at the supercharger.

Each set of records is made up of two photos, the lower one being observed with the cut-off knife edge vertical to accentuate shock conditions and the upper one with cut-off horizontal to accentuate boundary-layer conditions. This change in knife edge orientation is the reason for the fact that the shock systems in the upper pictures appear as black lines, whereas those in the lower pictures appear white.

It will also be noted that despite every effort to unify the flow across the cascade entry plane there is evidence of slight variations in velocity between passages. In the following analysis therefore, the uppermost passage has been considered, although identical conditions are to be seen in the other passages at slightly displaced speeds.

In Set 1 the presence of a series of small ' whisker ' shocks is to be seen near the blade leading edge on the convex surface. These shocks occur quite in accordance with theory for flow in curved channels, and they are accompanied by detachment of the laminar boundary layer from the blade surface with consequent wide wake originating early on the blade surface. The disturbed flow within this wake is discernible in the photographs.

These ' whisker ' shocks are also in accord with the findings of Ackeret, Feldmann & Rott[3] (1946) for shock development on a laminar boundary layer, and if their development is studied at later stages of flow they will be found to coalesce into a characteristic ' lambda ' shock system.

Set 2 of the photographs shows the gradual hardening of the wide wake boundary layer and the development of a compression region at the leading edge of the blade. There is also to be seen a slight expansion region at the blade trailing edge, whose later development should be noted.

In Set 3 the nose shocks have assumed a lambda formation, and the wake boundary layers have hardened sufficiently to create an effectively convergent flow passage, despite the geometrical divergence. This convergence permits regeneration of sonic conditions after the nose-shock breakdown, with the consequence that a second compression shock is formed well within the passage.

In Set 4 the second shock system has developed to a stage where its lower extremity may be seen to bifurcate, forming the characteristic lambda formation which indicates the probability that the boundary layer on the blade concave surface is laminar. The upper extremity, however, is single and merges into the turbulent wake boundary. This wake boundary may be seen to have

fallen back towards the blade surface as compared with earlier photos, and transition can be seen to be about mid-chord, despite the early detachment of the back face boundary layer by the nose shock.

Between the now fully developed nose shock, and the mid-passage shock may be seen a shockless compression region originating at the blade leading edge and extending across the effective passage throat. Very small shocks may also be seen just downstream of this region and forming on the concave side of the leading edge, from the presence of which it may be deduced that there is detachment of the laminar boundary layer on the concave side of the blade as well as on the convex surface.

It has been shown by Fage and Sargent[4] (1948) and others that the assumption that bifurcated shock and laminar boundary layer always occur together is incorrect. Nevertheless it is suggested that for the order of velocity here under consideration the probability that bifurcated shock indicates laminar boundary layer is a reasonable deduction.

The expansion region characteristic of supersonic flow into a low-pressure region over a sharp edge (Ewald, Poschl and Prandtl[5], 1936) is now plainly visible at the blade trailing edge, and there appears to be sufficient regeneration even downstream of the blades to originate a further shock system beyond this region.

At this stage it is worth pausing to consider the shock configuration. We now have the following :—

(1) A minute shock at the leading edge characterised by boundary-layer breakaway.

(2) A fully developed compression shock at mid-passage of which the lower half is of lambda formation, originating on the concave surface boundary layer (probably laminar), and the upper half is single, originating on the convex surface turbulent boundary layer after transition.

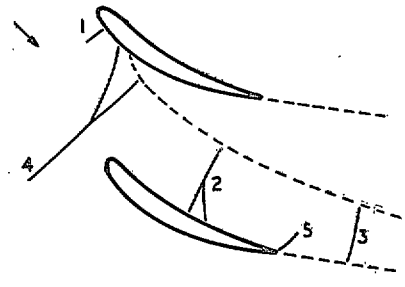

(3) A downstream compression shock produced by regeneration of velocity through the effectively convergent flow passage bounded by the blade wake.

(4) A fully developed and very stable lambda shock upstream of the passage throat, and evidently forming on a boundary layer which, though detached from the blade surface, may still be laminar.

(5) A Prandtl-Meyer expansion obliquely off the blade trailing edge and into the supersonic region between shocks 2 and 3.

In addition there is a shockless compression region in the passage throat between (1) and (2) and minute shocks visible on the concave side of the blade leading edge.

In Set 5 a quite definite and instantaneous rearrangement of shock becomes visible in the downstream part of the passage. Here shock 2 has progressed to the blade trailing edge where it merges with the expansion region to form the characteristic shock assembly for a supersonic divergent nozzle. The wake on the blade back face suddenly collapses and falls back on to the blade, whereat shock 4 reflects as an expansion diagonally across the passage from the convex boundary of the throat to the trailing edge.

Immediately ahead of this expansion there may also be noted a shock reflected from the rear branch of shock 4. This shock appears to reach across to the trailing edge of the next blade more clearly than the expansion, which is very much dispersed before it has extended far.

At this stage of the flow development the shock configuration may be depicted thus

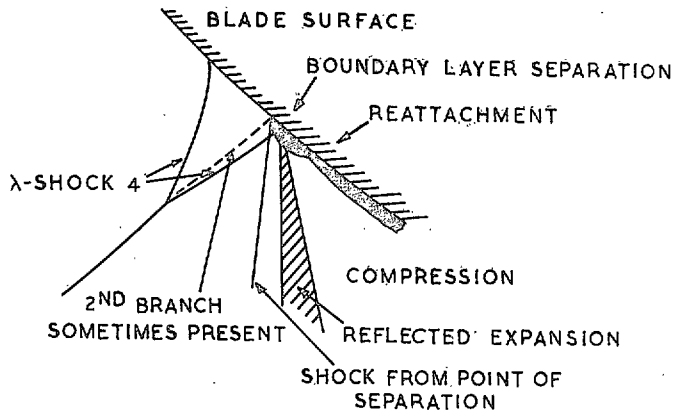

The reattachment of the separated boundary layer is linked with the deflection back to the surface of the streamlines at the foot of the incident shock and its reflected expansion.

The reasons behind this sudden re-orientation of shock must be associated with the maintenance of the general flow equations in an unstable flow region. The outcome is undoubtedly the sudden and vigorous reduction of the blade wake width and hence of the profile drag, accompanied by the formation of a well-defined shock system between the blade trailing edges.

It is significant that not until the changes just related, and recorded in view 5, occur, does the cascade inlet velocity reach its limiting value, at an impeller speed of 18,000 r.p.m.

At still higher impeller speeds no marked alterations have been noted although a general sharpening of the wave fronts is to be seen. The downstream shock formations assume the cruciform shape typifying supersonic discharge from a divergent nozzle and the profile drag is palpably low as evidenced by the almost complete disappearance of the wake. There must obviously be, however, a considerable energy loss through the intense shock systems at the passage outlet.

(*Note :* The dark patches to be seen in view 6 near the passage exit were produced by accumulation of foreign matter on the glass walls of the tunnel at these high flow conditions, and may be disregarded).

Two-Dimensional Loss and Deviation Tests.—In Fig. 5 have been tabulated the principal observations and calculated data showing the variations of inlet and outlet Mach numbers, velocities, pressure ratios, Reynolds numbers, losses, etc., obtained by traverses at mid-passage height.

At the bottom of this summary sheet have been noted the speed conditions at which the various special tests were carried out.

Derivation of the various calculated functions has been shown in the Appendix, but it may be accepted that deviation and deflection have their usual meanings, and loss has been expressed as percentage of the inlet velocity head, the units being converted from pressure to heat to conform with turbine engineering practice.

Reynolds number has been expressed here in terms of mean inlet velocity and blade chord, with kinematic viscosity corrected for change in density and temperature.

Fig. 6 shows all the relevant data of Fig. 4 plotted against impeller r.p.m. as abscissa. This abscissa was chosen deliberately for reasons already stated, but, as may be seen from its linear relationship to theoretical outlet Mach number (assuming no pitot-pressure loss) the use of this overall Mach number might equally have been selected.

In the plots shown in Fig. 6 it may be noted that high losses and deviation due to Reynolds number effects were visible at impeller speeds below 6000, which implied inlet Mach numbers below 0·3 and Reynolds numbers below $1{\cdot}6 \times 10^5$. In this range the pressure ratio across the cascade barely attained a value of unity.

At impeller speeds between 6000 and 10,000 r.p.m., or inlet Mach numbers 0·3 to 0·65 the loss and deviation values were at their lowest, being respectively of the order of 3·5 per cent and 10 deg. Pressure ratio rose gradually over this range to a maximum value of 1·095.

At just above 10,000 r.p.m. of the impeller, or at a Mach number of 0·65 the loss and deviation soared to approximately 30 per cent and 21 deg by reason of the advent of shock 1 in the blade passages, with consequent boundary-layer detachment.

At about 16,000 r.p.m., coincident with the sudden changes in shock formation already described, there was found to be a marked reduction in the mean deviations from 21 deg to 18 deg. This fall in deviation, indicating a reduction in the wake width beyond the blades, occurred just at the point where pressure ratio across the cascade fell once more to less than unity.

At 18,000 r.p.m. of the impeller the inlet Mach number became constant at 0·91, the critical value, the deviation having risen again to 20 deg.

At speeds above this critical value there became evident in the pitot traverses the advent of a second trough between those associated with the blade wakes. This trough increased in depth and width with speed increase, while the normal wake trough became less in width. The secondary trough was caused by loss through the shock which by now spanned the blade passage outlet, and it was possible, by assessing the proportions of the wake and shock trough relative to the inclusive loss, to show that at speeds beyond the critical value the profile loss began to fall rapidly, although the shock loss correspondingly increased to maintain the inclusive loss at the very high value of 40 per cent.

In this high-speed region the deviation also showed signs of falling again although the supercharger limitations permitted only one test result above 20,000 r.p.m. At these limit conditions also, the pressure ratio across the cascade was down to 0·8, so that no overall compression was available despite pressure rises through the shock systems. In fact of course, the best compression obtained at the upper limit of the low loss working range, *i.e.*, at inlet Mach number 0·65, a value only 71·5 per cent of the critical Mach number.

Fig. 7 shows calculated contraction coefficients and total percentage boundary-layer suction quantities over the test range, as an aid to assessment of the general validity of the tests from a performance standpoint. Contraction coefficients, or the ratio of the inlet to outlet axial velocity components were evidently rather lower than could have been wished for inside the low-loss range, but at the high-velocity range where most testing was carried out they were close to unity. They are of course materially affected by the amounts of boundary-layer suction applied.

Fig. 8 shows plots of observed pitot pressures and deviations at five impeller speeds chosen to represent the especial peculiarities found in the flow characteristics. Here the very considerable increase in wake width once shock has developed, is indicated in the test at 14,000 r.p.m. The 14,000 and 16,000 r.p.m. tests show the changeover to reduction in wake width and deviation value at this stage of the flow, and the 21,000 r.p.m. test indicates clearly the development of a secondary trough between the wakes, together with still further reduction in wake width. The secondary trough is also supported by a like peaking in the deviation traverse at that speed.

Three-Dimensional Loss and Deviation Tests.—The five representative speeds of 4000, 8000, 14,000, 16,000 and 21,000 r.p.m. of the impeller were again used for pitot-yaw traverses at heights other than mid-height so that an integrated loss over the full passage area, representative of the three-dimensional losses, might be obtained for comparison with the mid-height losses as representing the two-dimensional losses.

In Fig. 9 are shown loss and deviation contour plots for these five test speeds. Here the black areas show the regions of high loss (over 50 per cent) and deviation (over 20 deg) and the light regions the lowest loss values of 0 per cent and deviations below 10 deg.

It is convenient when considering these results to regard the passage height as divided into upper, middle and lower thirds. It is at once evident that the greatest changes occur in the middle third, the upper and lower third being largely within the downstream floor and roof boundary layers and therefore in a relatively low-velocity stream throughout the test range.

Consider first the low-velocity test where the two-dimensional loss was high due to low Reynolds number.

It will be seen that the mid-height loss is of the same order as that at all other heights, but the flow generally shows a lack of formation if compared with the higher speed tests. The deduction here is that the lack of entry air velocity and mass was such that the passage was not flowing full and there was therefore little persuasion for the air to follow the blade contours. In other words laminar-flow regions had not yet developed on the passage boundaries and so losses and deviations were still high. In fact the mid-height, or two-dimensional loss was still 100 per cent of the integrated three-dimensional loss, both being of the order of 17 per cent of the inlet velocity head.

In the second series at 8000 r.p.m. impeller speed the upper and lower-thirds of the passage have remained at fairly high loss, but the middle-third loss is much reduced by reason of the closure of the wake onto the blade back face and the large area of zero pitot loss. As a result of this configuration there is apparent a marked ' warping ' of the peak-loss trace away from the blade edge as the trace point is moved away from the passage mid-height. This warping is a characteristic of compressor cascades in the working range, and can be associated both theoretically and practically with the ' downwash ' consequent upon secondary-flow considerations.

At this stage, in the middle of the cascade working range the two-dimensional loss of 4·2 per cent is only 25 per cent of the three-dimensional integrated loss of 17·1 per cent, which incidently remains at the same approximate value as that for the low-velocity test series.

Before leaving this 8000 r.p.m. range it is interesting to note how closely the deviation contours support the configuration of the loss contours.

Consider now the two tests at 14,000 and 16,000 r.p.m., just before and just after the shock-wave re-orientations already discussed in the optical tests.

Here again it is in the middle-third that the greater changes are evident, and as might be expected with the two-dimensional loss already of the order of 30 per cent, it is in the deviation changes the most interest is found. The two-degree fall in mid-height mean deviation at the higher test speed is supported by the increase in the low deviation area between the blades. Otherwise there is little difference between the two test series and the two-dimensional losses of 28·1 per cent and 35·3 per cent are respectively 83 per cent and 91 per cent of the three-dimensional loss evaluations. The characteristic warping has entirely disappeared.

Finally at the top speed test series the secondary loss due to shock formation has become clearly evident and extends over the full middle-third of the passage height. It is only between the critical speed of 18,000 r.p.m. and the top speed of 21,000 r.p.m. that this secondary trough develops and it increases not only in width across the passage but also in height of passage. It is supported by an increased deviation region.

The ' warping ' of the peak loss traces at different stages in the test range has already been referred to but it is made more clear by plotting, as in Fig. 10 the relative positions over passage height of the minimum points reached in the loss trough in one passage at each traverse position. In the top-speed test this same technique has also been applied to the shock-loss trough as shown by the broken line.

Secondary Flow Investigation.—As a result of deductions inspired by the tests so far considered, and of arguments set forth by Carter[6] (1948), it was thought desirable to attempt the observation of secondary-flow vortices, and/or trailing vortices in the wakes of the test cascade at some of the representative speeds chosen.

To this end the swirl vane already referred to was developed, and yielded interesting results.

Before considering these results, however, it may be of use to refer briefly to the theory underlying this part of the test programme.

In Fig. 11 is drawn a perspective diagram of the secondary-flow conditions prevailing in a cascade of blades where the roots and tips are bounded by floor and roof walls. It is well known that when flow takes place through a system of curved channels the resultant centrifugal forces on the air must be balanced by pressure gradients in which the pressure falls towards the inner side of the bend, *i.e.*, towards the convex blade surface. Since, however, the velocities of flow are reduced near the floor and roof walls by reason of boundary-layer build-up, the centrifugal forces and pressure gradients will be less near the walls than at the blade mid-height. This variation over height results in the formation of systems of vortices V within the blade passages.

These vortices V will persist independently in each passage of the cascade until such time as they meet at the blade trailing edges. Here they bring about a discontinuity of velocity which results in a vortex sheet at the blade edges. In the course of its movement downstream this unstable vortex sheet rolls up to form a new system of vortices W within the blade wakes. These are consistent with the trailing vortices which would be expected if the cascade be considered as a system of single aerofoils undergoing normal aerodynamic flow.

Whether or not the original vortices V be considered as inducing or being induced by the trailing vortices W is a matter for argument, as also is the possibility of their continuing to exist at some distance downstream of the blades, in the form of vortices V_1.

Now it will be noted that the result of the vortex pairs W on the flow downstream of the cascade is tending to reduce the deviation at blade mid-height and increase it near the root and tip, whereas that of the systems V_1 (if still existing) would be in the opposite sense.

In practice, as has already been shown in the deviation contour plots, there is a marked deviation reduction at blade mid-height within the low-loss flow range, and it seems clear that this is due to the downwash of the trailing vortices W.

In Fig. 12 are shown contours of constant swirl-vane r.p.m. which were observed in a plane one chord beyond the blades when viewed from upstream. The tests were made at 3 velocities corresponding to high loss from low Reynolds number effect (4000 r.p.m.), low-loss high-efficiency conditions (8000) and high loss due to shock effects (20,000).

It will be immediately seen that at the low-loss test speed there existed a definite system of vortices consistent with those marked W in the diagram in Fig. 11, with evident downwash at blade mid-height. Comparison of this vortex plot with the appropriate loss contour plot in Fig. 9 shows a like warping in the flow.

Similarly, in the low-speed test the multiple system of small vortices (although still consistent with those marked W and still showing downwash) indicates a lack of conformity of the flow consistent with its not having achieved the full controlling effect of the passage bounding walls.

At the high-speed end of the test range, a considerable number of tests were made in an endeavour to trace vorticity after the advent of shock. As is shown however, little or no vorticity was detectable above impeller speeds of 11,000 r.p.m., and that which was found was well out towards the blade roots and tips.

Two practical details of the swirl-vane tests may here be noted. The first is that physical size of the instrument prevented observations as near to the floor and roof walls as could have been desired, and the second is that although in theory the vane r.p.m. over the whole field of a vortex should remain constant, it was found possible in practice to locate the core of the vortex by plotting iso-speeds around the highest measured position, as had been done in the figure.

A third point was the fact that with very high air speeds there was a tendency for the axial thrust on the swirl vane to reduce its freedom of rotation, and this fault was thought to be a possible reason for the apparent lack of vorticity in the critical-flow test. The vane was found to be still free when exposed to a full sonic velocity air jet in the open atmosphere, and as has already been stated, a considerable number of tests were made before it was concluded that vorticity of measurable intensity was non-existent at the high-speed end of the range.

Summary of Flow Characteristics.—In Fig. 13 an attempt has been made to depict the various stages of development of the flow in this test cascade in the light of the several researches above reported.

In view of the limitations in respect of aspect ratio and maximum air speed it would be imprudent to generalise too broadly, but it is thought reasonable to suggest that for aspect ratios of the order normally considered in compressor design these flow characteristics may be encountered.

In the first place, it must be appreciated that optical analyses show only the cross-sections of shock-wave developments. But since shock must develop over an area of flow which has height as well as width, it is essential to consider loss contour plots as well as shock analyses for a full understanding.

It would seem then that for this aspect ratio it is chiefly the middle-third of the flow passage which is affected by shock developments, with a tendency to increase to the middle-half once fully developed shocks are existing.

The expansion in height of such shock systems as do occur means that the velocity in front of them also tends towards uniformity over height, and the physical characteristics underlying secondary flow and trailing vortex development are forced outwards towards the blade roots and tips. This hypothesis explains the inability to detect trailing vortices at the high-speed end of the test range, and the lack of warping in the loss and deviation contours, consequent upon lack of downwash.

Referring again to Fig. 13, sketch 1, shows approximately the wake distribution over blade height due to Reynolds numbers and velocities so low that the air is not yet constrained to the blade boundaries. Consistent with this explanation are the numerous indeterminate vortices apparent in the wake.

Sketch 2 shows how as inlet air speed and Reynolds number rises the trailing vortices become well defined and bring with them marked downwash which induces low loss and deviation in the middle-third of the passage, with consequent discrepancy between two and three-dimensional loss evaluation, and warping.

Sketch 3 indicates by the shaded area near the convex leading edge that shock has just been achieved. The consequence is to raise the loss in the middle-third, by reason of wake boundary-layer detachment, and thence to force the trailing vortices, out towards the blade root and tip sections. Warping disappears and two-dimensional loss begins to approach the three-dimensional value.

In Sketch 4 shock has developed to the stage of four compression shocks in series, two being of a lambda pattern, and the middle-third loss has developed still further towards the three-dimensional value. It is surmised also that the trailing vortices are still further relegated to the blade root and tip regions.

In Sketches 5 and 6 are two stages of the shock development where flow has been once again forced back on to the convex blade surface by reason of the diagonal expansions originating at the sharp trailing edges. The result is a general reduction in wake width, plus a gradual increase of shock loss, so that although profile-drag loss is being rapidly reduced, inclusive loss remains high.

It is believed that were the downstream pressure to be still further reduced a fourth stage of shock would develop where typical supersonic nozzle shock characteristics would become visible. This stage however was beyond the scope of the power plant in these tests.

As a result of this detailed flow study it was concluded that by delaying the advent of the initial whisker shock until the inlet velocity to the blading was closer to the critical value, and by also so designing the passage that for zero incidence the contraction ratio was not less than unity, it might be possible to improve both the high sub-critical cascade performance and reduce the shock loss when it occurred.

As means to this end a blade was constructed in which the leading edge was sharp, the maximum thickness was displaced to 50 per cent chord as compared with 32·6 per cent for the conventional section, and the thickness/chord ratio reduced from 11·04 per cent to 8·1 per cent. The stagger was maintained at — 30 deg for both sections, but the camber of the experimental section was so reduced that for zero incidence the contraction ratio was near unity.

Test Data. Part 2.—*Optical Tests.*—In Fig. 14 are shown reduced photographs of the complete set of schlieren records. They are set out so that study from left to right shows the effect of increasing inlet velocity at constant incidence, and study from top to bottom shows the effect of decreasing incidence, and hence of increasing contraction ratio at constant impeller speed. This does not mean constant inlet velocity, however, for which comparison it is necessary to follow a diagonal line from top left to bottom right of the set of pictures.

Although much may be learned from a close study of these photographs it is thought perferable to discuss in detail a few selected pictures which will be found full-size in Fig. 15. They show from top-left to bottom-right the effect of decreasing incidence and increasing contraction ratio for an inlet velocity which is of the order of 90 per cent of the critical value. From bottom-left to top-right is shown the effect of increase of inlet velocity from 60 per cent of critical up to 100 per cent of critical with constant incidence.

Considering first the constant-incidence records C1, C3 and C6, it will be seen that shock is not initiated until some 80 per cent of the critical entry velocity, and that it then forms at the point of maximum thickness of the blade and not near the leading edge as was the case for the conventional section.

Shock brings with it the familiar boundary-layer detachment on the back of the blade with consequent profile-drag increase, as shown by the wake width increase in C3. As shock develops a simple normal shock-wave first spans the passage and later moves down to the trailing edge, forcing the wake back on to the blade and forming a characteristic cruciform system downstream of the passages. The passage itself is left with a fairly weak system of simple oblique shocks.

Comparison of this shock system with that for a conventional blade under similar operating conditions shows that there is much less complication in the flow and the assumption that simplification brings with it reduction in shock loss is supported by the pressure traverse tests.

It should be remembered here that zero incidence on this cascade includes a contraction ratio of unity.

If now the pictures A3, C3 and E3 be studied one sees immediately that positive incidence (A3) brings with it a contraction ratio of less than unity (0·84) and a strong shock system upstream of the passage throat with an extension across the inlet section from each successive blade. In fact the range of pictures at + 10 deg incidence bears a close resemblance in form and complexity to those taken of the conventional cascade.

The improvement in shock pattern brought about by increasing the contraction ratio to unity is clearly shown by comparing A3 with C3.

Photo E3 and others in the — 10 deg incidence group show the price that must be paid for reducing the curvatures at the blade leading edge by applying sharpness. Here the incidence is such that a stall is precipitated on the concave surface of the blade even before shock occurs, and then the arrival of shock adds further to the profile drag by the shock stall on the convex surface.

It may be concluded from study of the shock photographs that the design premises of this experimental section are justified, and that the salient features to be aimed for are sharp nose, maximum thickness well back along the chord, medium camber and curvature of the blade surface, and contraction ratio not less than unity within the working range of incidence. The disadvantages of these features may be expected to be a fairly severe limitation in working range of incidence and some reduction in blade strength, but performance at high entry velocities may be expected to be better than that of a conventional section.

Performance Analysis.—Proceeding now to the quantitative examination of cascade performance by wake pressure traversing, the full summary of observations and calculations is given in Fig. 16.

The various calculated characteristics have been obtained by methods shown in the Appendix, and the shock photographs have been associated with their appropriate pressure tests by the key added at the bottom of the tabulation.

In Fig. 17 are plotted the contraction coefficients for each test, and the total boundary-layer suction quantities as percentages of the inlet mass flow. These plots serve as an indication of the tunnel conditions prevailing for any given test, and they are seen to be reasonably satisfactory. The low-speed tests tend to permit removal of rather more boundary layer than is advisable, although this condition is usually conjunct to the establishment of the entry conditions, and its effect on the contraction coefficient does not seem to be unduly marked.

Fig. 18 shows the estimated performance of this cascade for all five test incidences. From these curves it will be seen that the working range of incidence is from + 5 deg to at least — 5 deg, a not unsatisfactory range, and that within this range losses are of the order of 3 per cent of the inlet velocity head and deviations of the order of 2 deg.

At negative incidences the pressure rise available across the blading, as shown by the pressure ratio plots, is very small, but at increasing positive incidence it is at peak quite satisfactory.

Reynolds number effects appear at values less than approximately 15×10^4, which correspond to inlet Mach numbers for this blade chord of the order of 0·3.

Shock stall becomes evident from the increase in loss at Mach numbers in the region of 65 per cent of the critical value, but pressure ratio is still available without prohibitive shock loss up to Mach numbers as high as 91 per cent of the critical Mach number. Moreover, the advent of shock does not appear to increase loss nearly so precipitately for this blade as for the conventional section. Even under fully developed shock-stall conditions the total-head losses are of the order of only 20 per cent in the working range, as compared with 40 per cent in the conventional cascade.

The loss and pressure-ratio characteristics have been replotted in Fig. 19 as a three-dimensional graph so that the working range of incidence and inlet Mach number may be more clearly assessed. Here the working range has been limited to that region where the loss is not greater than 5 per cent. If 6 or 7 per cent loss be permitted the working range of entry velocity is considerably increased, as also is the available peak pressure-ratio.

Finally, in Fig. 20, is shown a comparison of the loss, deviation, and pressure-ratio characteristics at zero incidence for this blade section and the standard RAF. 27 + 10 per cent section. Here it may be seen that despite considerable reduction in camber the experimental blade maintains the same peak pressure-ratio as the conventional blade with a somewhat better ratio at the low-speed end of its range, but with a lower value in the low-loss region.

The peak pressure occurs at 91 per cent of the critical entry Mach number, and a loss of 13 per cent for the experimental blade as compared with 75 per cent of critical Mach number and 20 per cent loss for the conventional blade.

Deviation for the experimental blade is 2 deg as compared with 10 deg in the working range, and maximum loss, fully shock stalled, is 20 per cent as compared with 40 per cent. The increase of loss with increasing shock loss is also considerably less severe.

At the low-speed end of the range, Reynolds number effects become apparent at the same value for both sections.

Conclusions.—Arising from these two research programmes, and bearing in mind that many variables are involved both in regard to the blade shapes and the passage shapes defined by the orientation of the blades, the following conclusions are drawn :—

(1) That even for aspect ratios of 2 the two-dimensional losses in a cascade are approximately equal to the three-dimensional losses at all test speeds except those in the high-efficiency working range. In this range the two-dimensional loss is roughly 25 per cent of the three-dimensional loss.

(2) That operation beyond the critical inlet velocity of a cascade can induce marked reduction in profile drag from the blades, although such advantage may be lost by the advent of shock losses.

(3) That shock loss within the critical-flow region may be delayed or reduced, thus reaping benefit from reduced profile drag in this region, by ensuring that the compressor blade and passage design includes the following :—

(*a*) Sharp leading edge and shallow curvature, particularly in the leading-half of the section.

(*b*) Maximum thickness in the region of 50 per cent chord and not greater in dimension than 10 per cent chord.

(*c*) Medium camber with pitch/chord ratio of the order of 0·8.

(*d*) Stagger and incidence chosen so that contraction ratio does not fall below unity.

(4) That improved high-speed performance by the above means will probably involve reduction in working incidence range.

Acknowledgment.—The author thanks the Metropolitan-Vickers Electrical Company Limited, and the Ministry of Supply for permission to publish these researches, and acknowledges the assistance given by the staff of the Aerodynamics Division of the National Physical Laboratory in the interpretation of some of the results.

REFERENCES

No.	*Author*	*Title, etc.*
1	K. W. Todd	Practical Aspects of Cascade Wind Tunnel Research. *Proc. I. Mech. E.*, Vol. 157, p. 482. 1947.
2	K. W. Todd	Some Developments in Instrumentation for Air Flow Analysis. *Proc. I. Mech. E.*, Vol. 161, p. 213. 1949.
3	J. Ackeret, F. Feldmann and N. Rott	Investigations into Compression Shocks and Boundary Layers in rapidly moving gases. *Mitteilungen aus dem Institut für Aerodynamik.* Zurich. No. 10. 1946.
4	A. Fage and R. F. Sargent	Shock-Wave and Boundary-Layer Phenomena near a Flat Surface. *Proc. Roy. Soc.* June, 1947.
5	P. P. Ewald, Th. Poschl and L. Prandtl	*Physics of Solids and Fluids.* Ch. VII. Blackie & Son, Ltd., London. 1936.
6	A. D. S. Carter	Three-Dimensional Flow Theories for Axial Compressors and Turbines. *Proc. I. Mech. E.*, Vol. 159, p. 255. 1948.

APPENDIX

Calculation of Performance Characteristics

Notation.

Ambient temp.	T	
Total pressure	P	Suffix $_0$ for inlet and $_1$ for outlet
Static pressure	S	
Air velocity	W	
Air inlet angle	α	To line of cascade
Air outlet angle	β	
Specific heat at constant pressure	K_P	
Specific heat at constant volume	K_V	
Ratio of specific heats	$K_P/K_V = N$	
Mechanical equivalent of heat	J	
Air density	ρ	

Derivations.

Mach number $= \sqrt{\left\{\frac{2}{N-1}\left[\left(\frac{P}{S}\right)^{\frac{N-1}{N}} - 1\right]\right\}}$

Overall Mach number $= \sqrt{\left\{\frac{2}{N-1}\left[\left(\frac{P_0}{S_1}\right)^{\frac{N-1}{N}} - 1\right]\right\}}$

Total-head loss $100\,\delta i/i$ as percentage

where δi is heat equivalent of pressure change $\delta P = P_0 - P_1$

and i is heat equivalent of pressure change $P_0 - S_0$.

These heat equivalents were derived from plotted relationships between $i_{1,2}/T$ and $\delta P/P$ for adiabatic expansion from conditions 1 to 2 where :—

$$i_{1,2}/T = K_P/J\left[1 - \left(\frac{P_2}{P_1}\right)^{\frac{N-1}{N}}\right]$$

$$\text{Pressure ratio} = S_1/S_0$$

$$\text{Contraction coefficient} = \frac{\text{Axial component of inlet velocity}}{\text{Axial component of outlet velocity}}$$

$$= \frac{\text{Theoretical axial component of outlet velocity assuming continuity of mass flow}}{\text{Observed axial component of outlet velocity}}$$

$$= W_0\rho_0 \sin\alpha / W_1\rho_1 \sin\beta$$

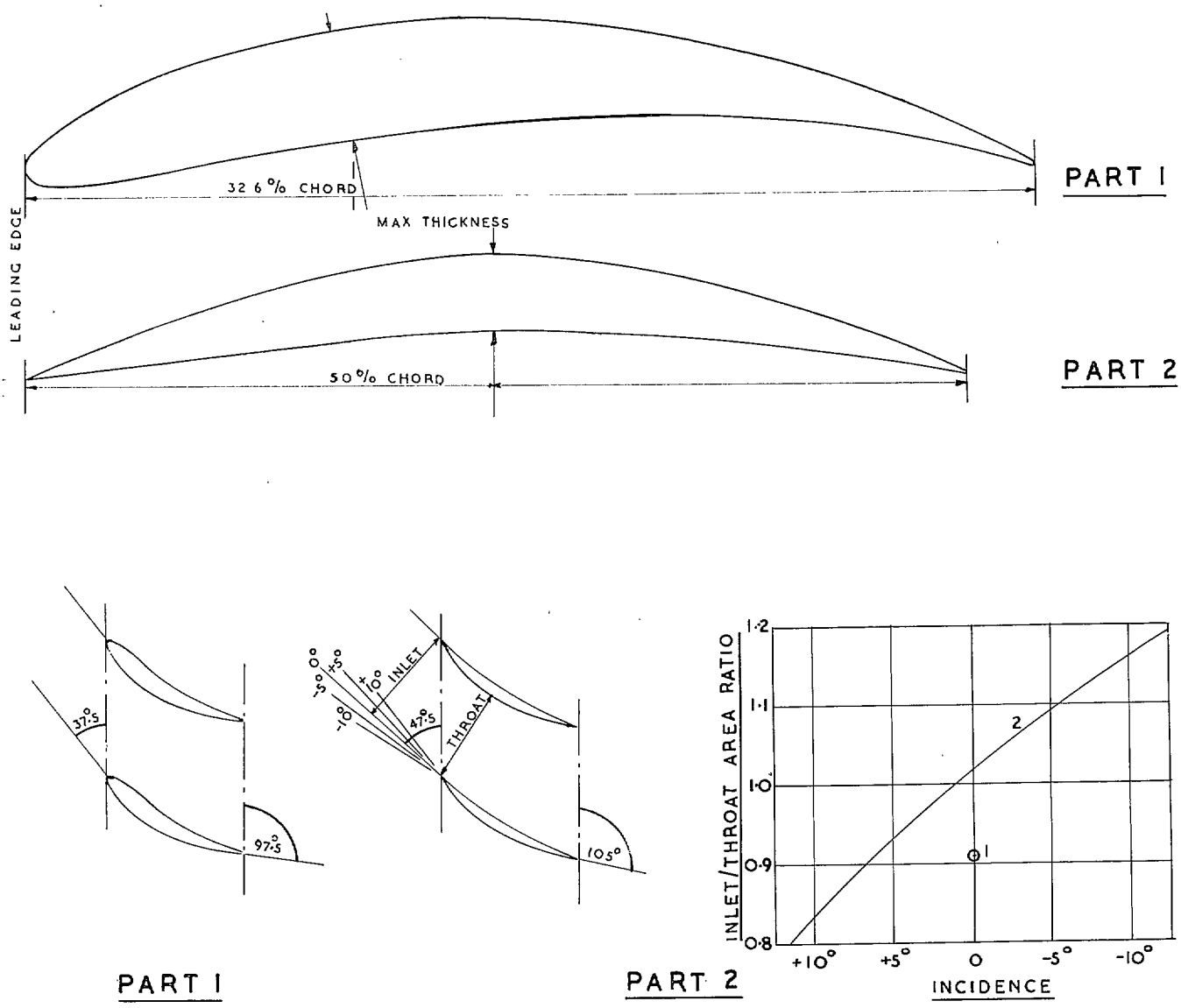

FIG. 1. Blade details.

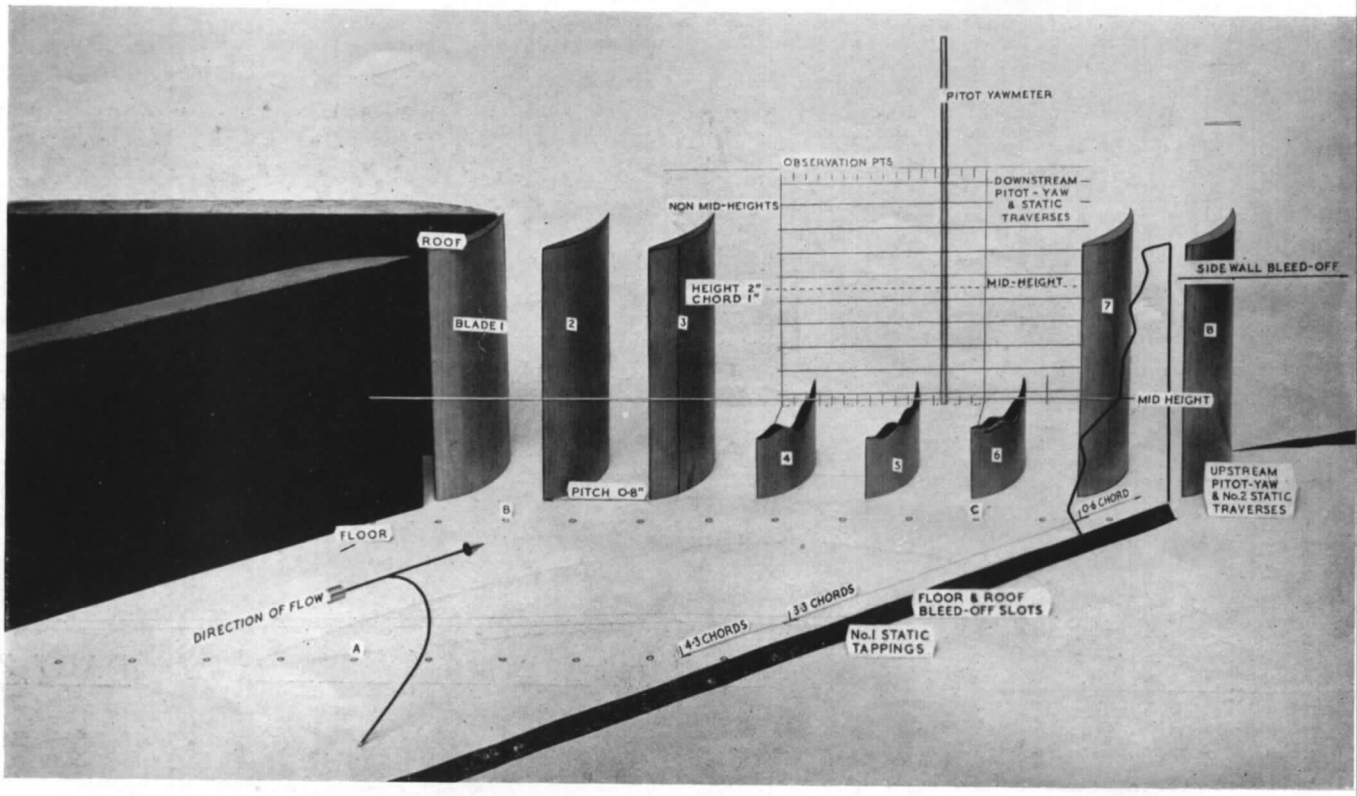

FIG. 2. Cascade assembly details.

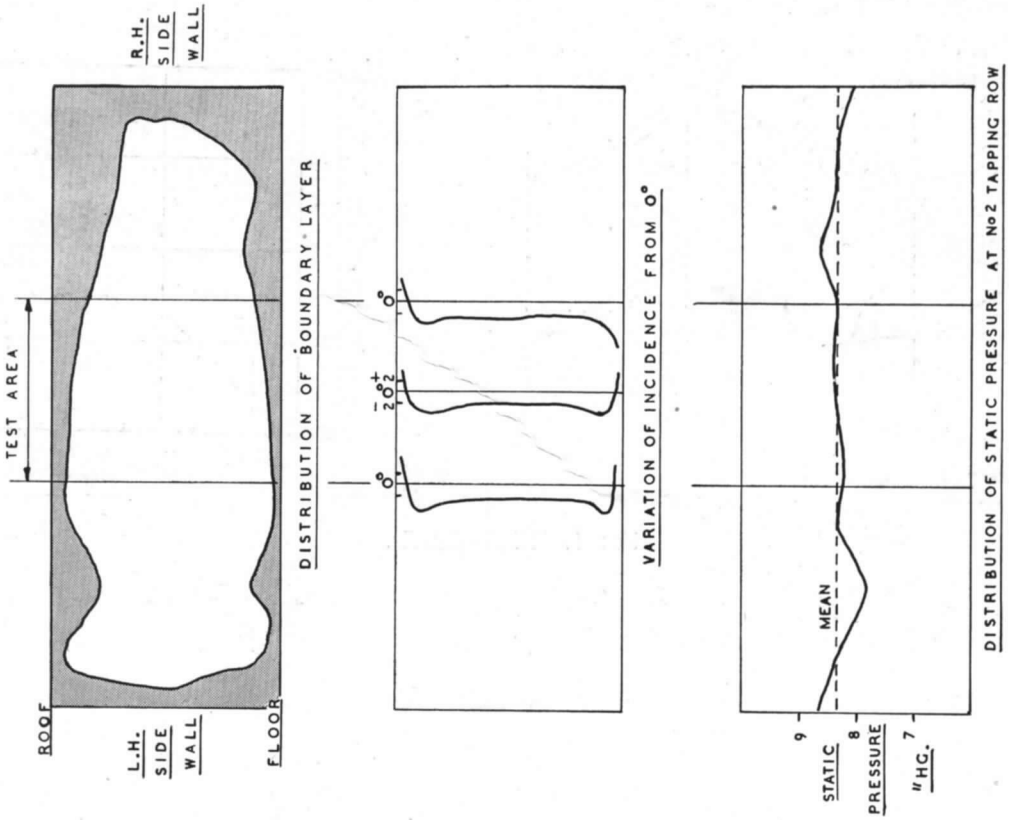

FIG. 3. Typical inlet conditions at Mach number 0·7.

To face p. 16

IFE
DGE

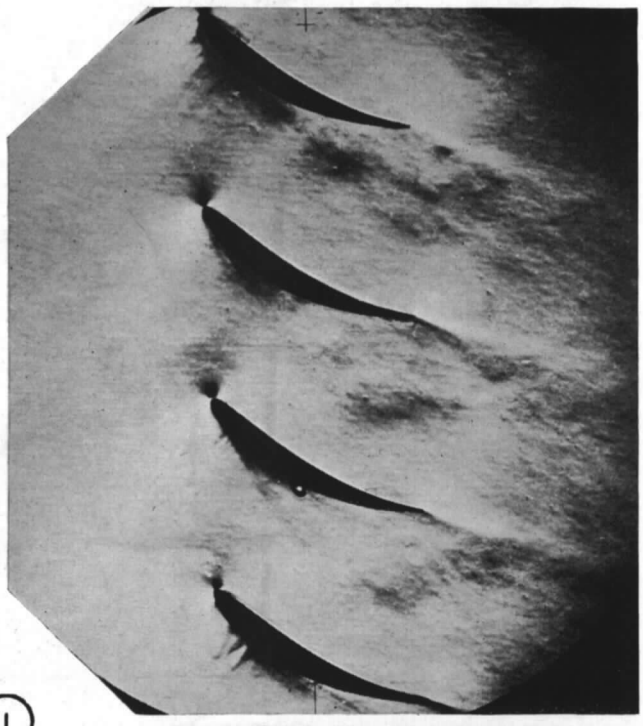

(1)

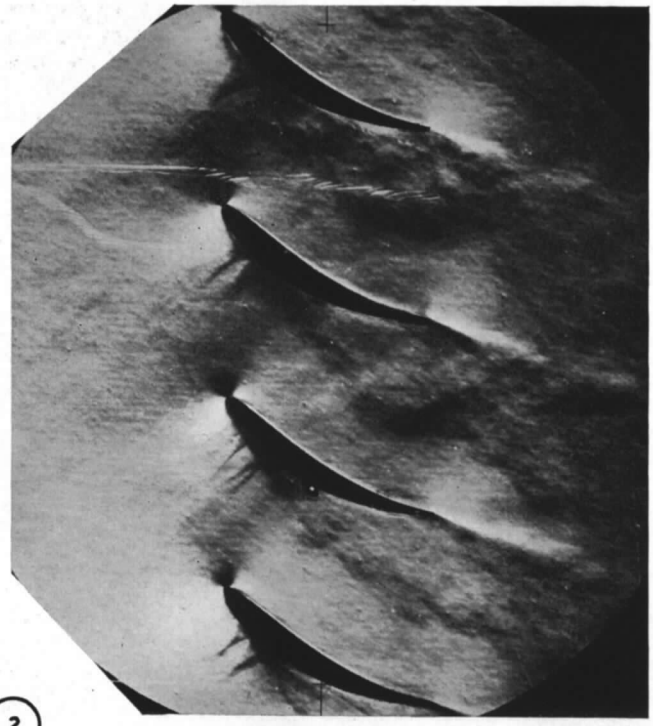

(2)

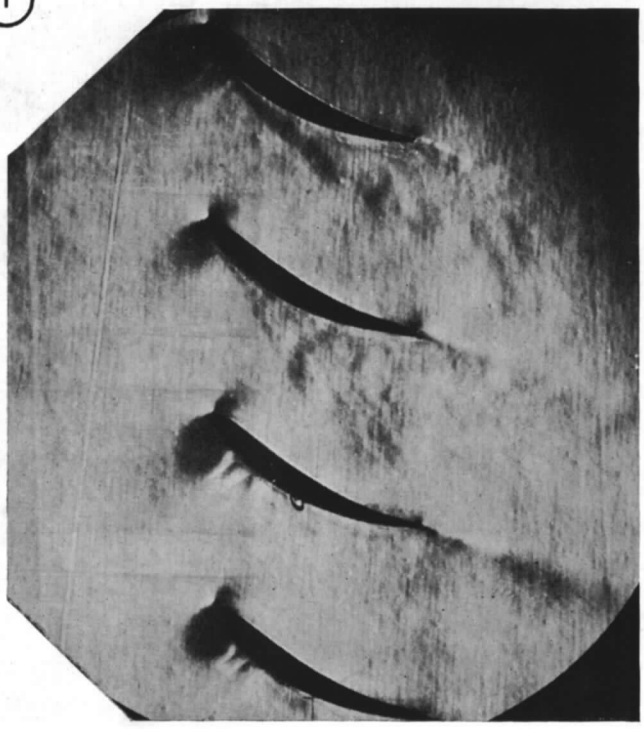

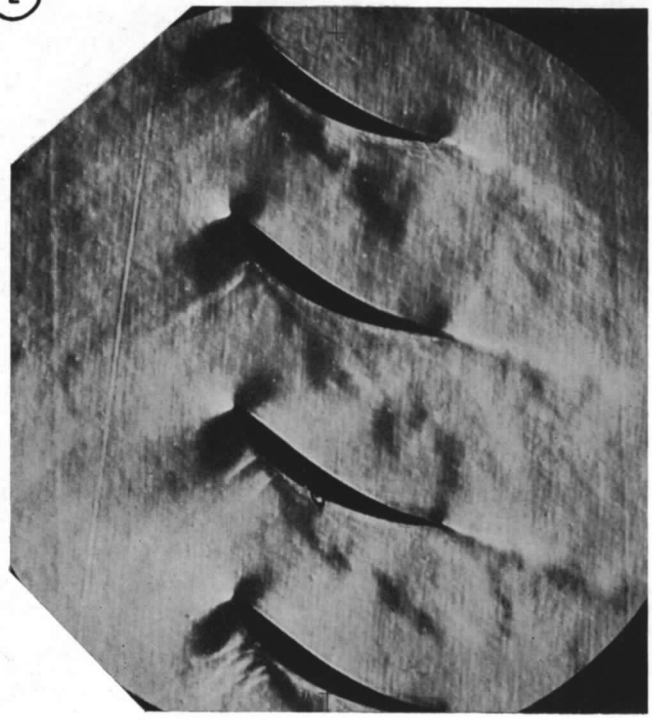

CH No. IMPELLER R.P.M. 0·63 10000 0·76 12000

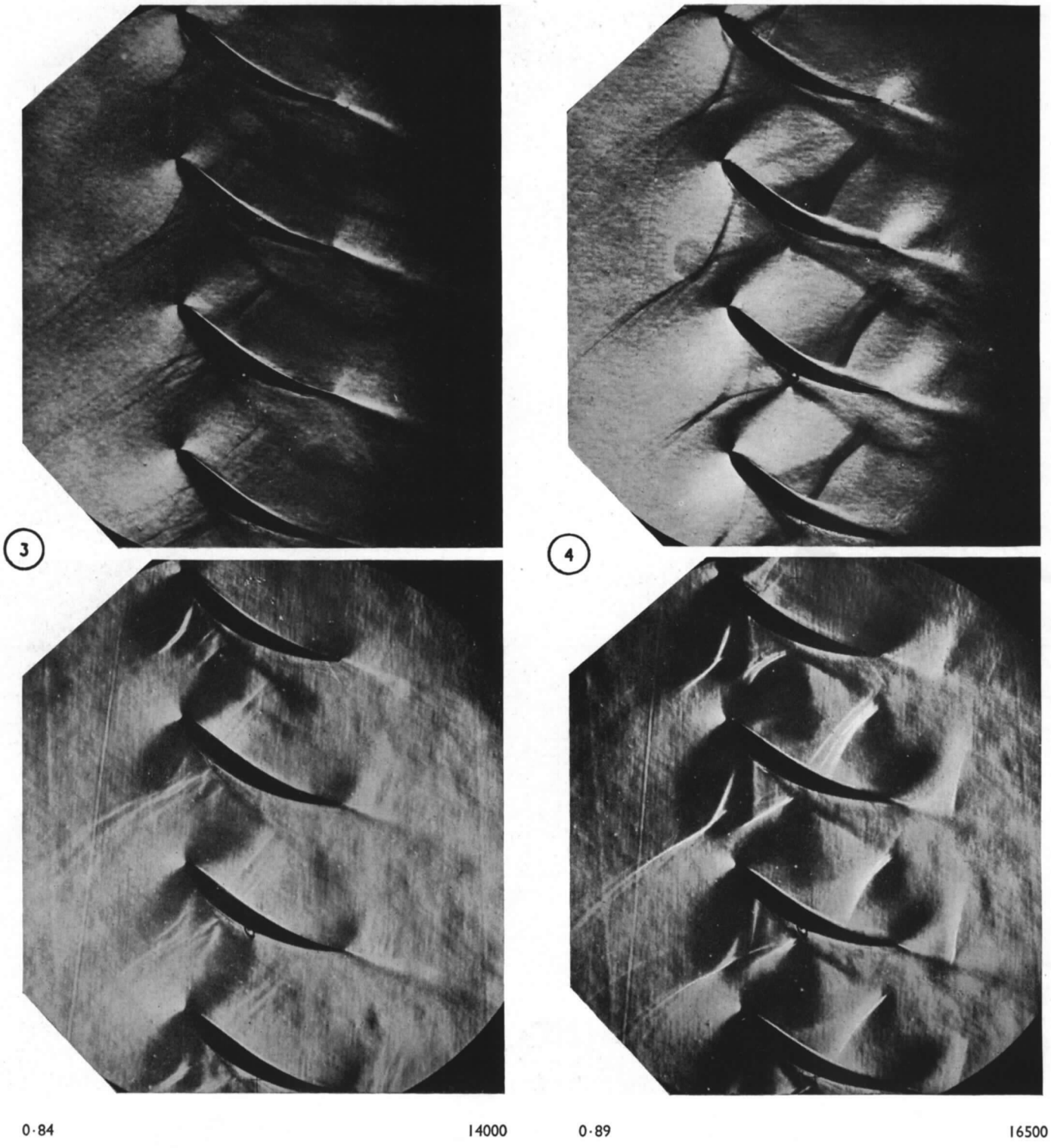

FIG. 4. Schlieren records of shock-wave development.

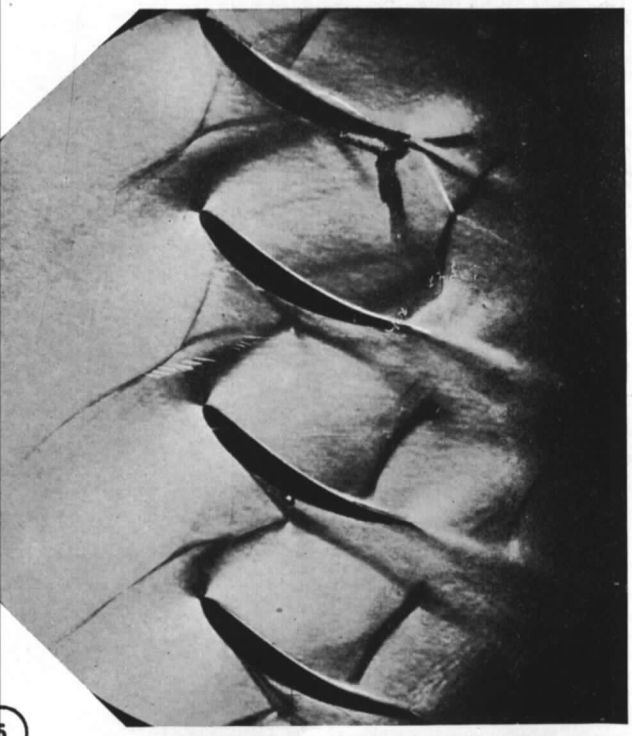

0·91 18000

(6)

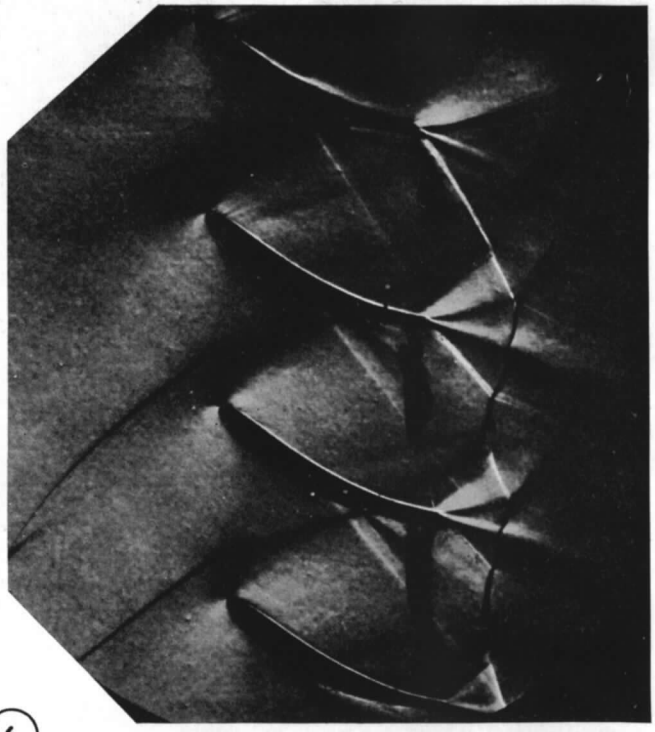

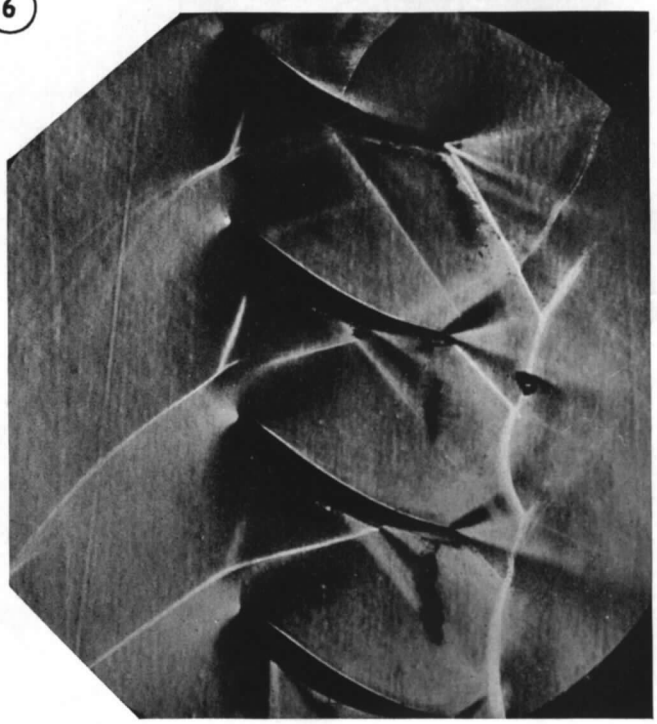

0·91 20000

CASCADE DETAILS

SECTION R.A.F. 27 + 10 %	PITCH/CHORD 0·8
CAMBER 45°	ASPECT RATIO 2
STAGGER −30°	NO OF BLADES 8
CHORD 1·0 INCH	NOMINAL INCIDENCE 0°
HEIGHT 2·0 INCH	MN. ACT. INCID. −2·5°
BLADE INLET ANGLE 37·5°	ROLLED BLADING
BLADE OUTLET ANGLE 97·5°	

TABULATION OF RESULTS PART I

1	TEST NUMBER		355	356	357	358	343	360	344	352	345	359	346	353	347	354	351	350	349	348
2	AMBIENT TEMP.	°C ABS	300	300	293	294	295	296	293	297	297	295	297	298	295	294	294	291	294	294
3	IMPELLER R.P.M.		EQ. 2500	EQ. 4000	5500	7000	8000	9000	10000	11000	12000	13000	14000	15000	16000	17000	18000	19000	20000	21000
	INLET																			
4	MACH NO.		0·125	0·207	0·316	0·420	0·503	0·560	0·648	0·697	0·750	0·800	0·830	0·855	0·871	0·910	0·912	0·910	0·911	0·911
5	VELOCITY	FT/SEC	140	234	349	463	549	611	695	751	803	847	882	901	916	955	951	945	950	950
6	REYNOLDS NO.	X 10^4	6·79	11·2	17·14	22·2	25·6	27·6	31·2	32·3	33·8	35·1	35·9	35·8	37·1	38·6	38·3	38·6	37·9	38·2
7	MASS FLOW	LB/SEC	0·479	0·789	1·173	1·496	1·720	1 845	2·015	2·062	2·180	2·210	2·262	2·225	2·262	2·360	2·305	2·335	2·345	2·345
	OUTLET																			
8	MACH NO.		0 101	0·160	0·175	0·354	0·401	0·465	0·515	0·503	0·505	0·565	0·597	0·640	0·680	0·732	0·770	0·836	0·880	0·905
9	VELOCITY	FT/SEC	114	181	195	391	438	511	560	552	554	616	650	694	730	783	818	876	920	942
10	DEVIATION	DEG.	21	16·5	9·9	10·4	10·9	9·5	10·2	14 9	17 6	20·5	20·6	18·4	17·6	18·1	20·2	20·8	21 8	20 2
11	DEFLECTION	DEG.	21 5	26	32·6	32 1	31·6	33	32 3	27 6	24·9	22	21·9	24·1	24 9	24 4	22 3	21 7	20 7	22 3
12	TOTAL HEAD LOSS	%	25·4	17·1	3·11	3·35	4·2	3 35	4 26	19·4	29 6	29·9	34	37·2	38·7	38 5	41 1	38 9	39 7	41 5
13	PRESSURE RATIO		0·98	1·005	1·02	1·03	1·055	1·063	1·092	1·093	1·088	1·08	1·055	1·017	0·986	0·97	0 922	0 872	0 833	0 806
	BLEED-OFF																			
14	LEFT SIDEWALL	%	1·500	1·605	1·350	1·390	1 700	1·160	1·475	0·822	0·832	0·612	0·585	0·342	0 730	0 702	0 870	0	0 678	0
15	RIGHT SIDEWALL	%	4·130	5·200	0·379	1·250	2·790	1·120	2;180	1 990	1·860	1·515	1 600	1 525	1 462	1 410	1 325	1 250	1 130	1 163
16	ROOF	%	2·010	1·930	2 440	1·780	0·613	2·220	0·410	1·390	0·810	0·860	0·730	0·993	0·585	0 565	0 556	0 765	0·845	0·785
17	FLOOR	%	2·582	2·090	2·680	1 950	0·363	2 350	0·348	1·330	0·820	1·000	0·754	0·900	0·570	0 547	0 320	0·865	1 160	0·580
18	TOTAL	%	10·222	10·825	6·849	6·370	5·466	6·850	4·413	5·532	4·322	3·987	3·669	3 760	3·347	3 224	3 071	2 880	3 813	2·528
19	CONTRACTION COEFF.		0·900	0·909	1 191	0·782	0·818	0·766	0·784	0·904	1 00	0·984	0·996	0·966	0·952	0 945	0 954	0 925	0 920	0·912
20	OVERALL MACH NO.		0·120	0·196	0·270	0·365	0·418	0·475	0·530	0·591	0·653	0·720	0·775	0·837	0·885	0·935	0 985	1 010	1 050	1 070
	SPECIAL TESTS																			
	OPTICAL																			
	YAWMETER																			
	3 DIMENSIONAL LOSS	%		1·686			17·00						28·1		353					42·3
	SWIRL VANE																			

FIG. 5

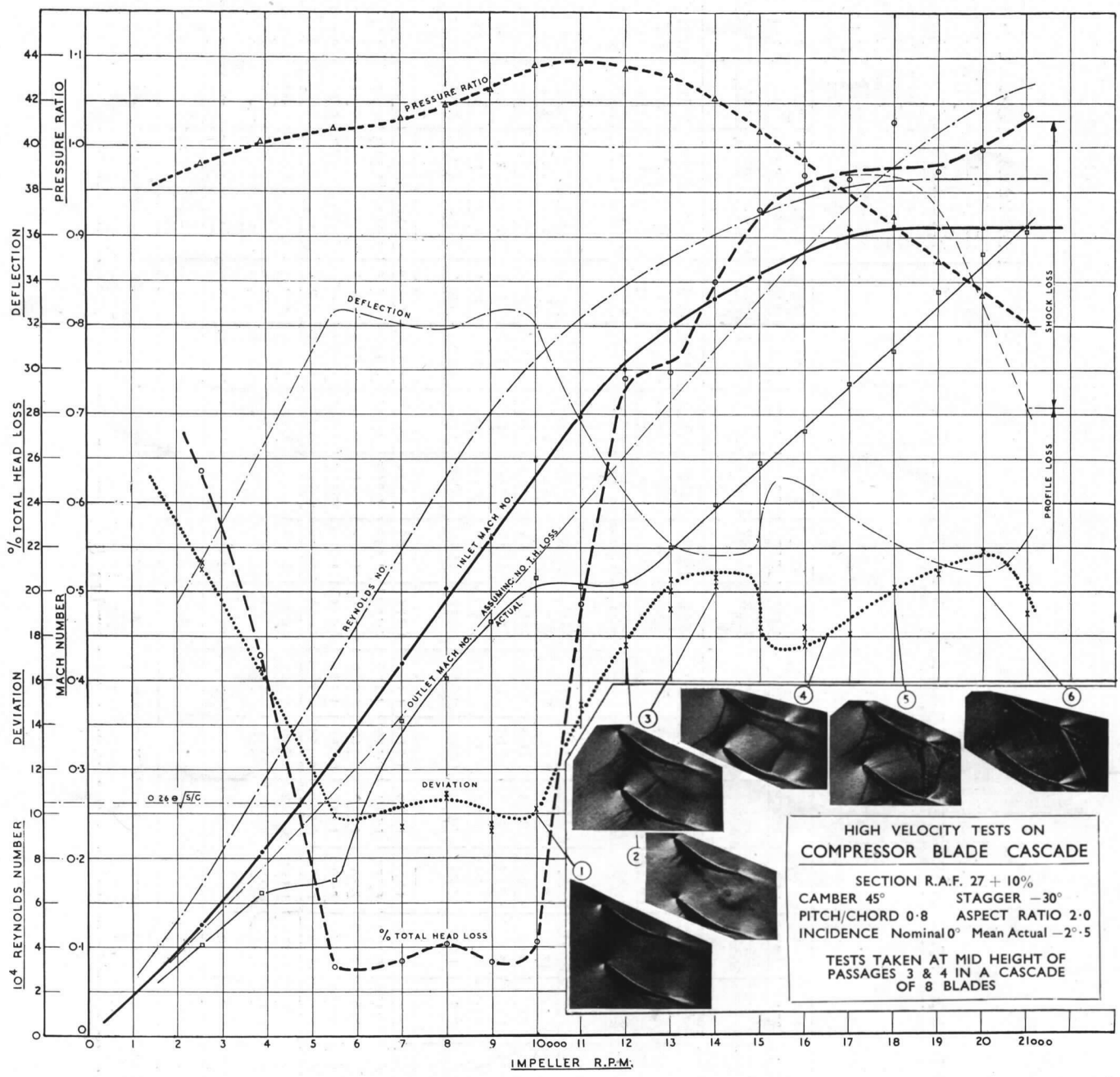

FIG. 6. Performance characteristics.

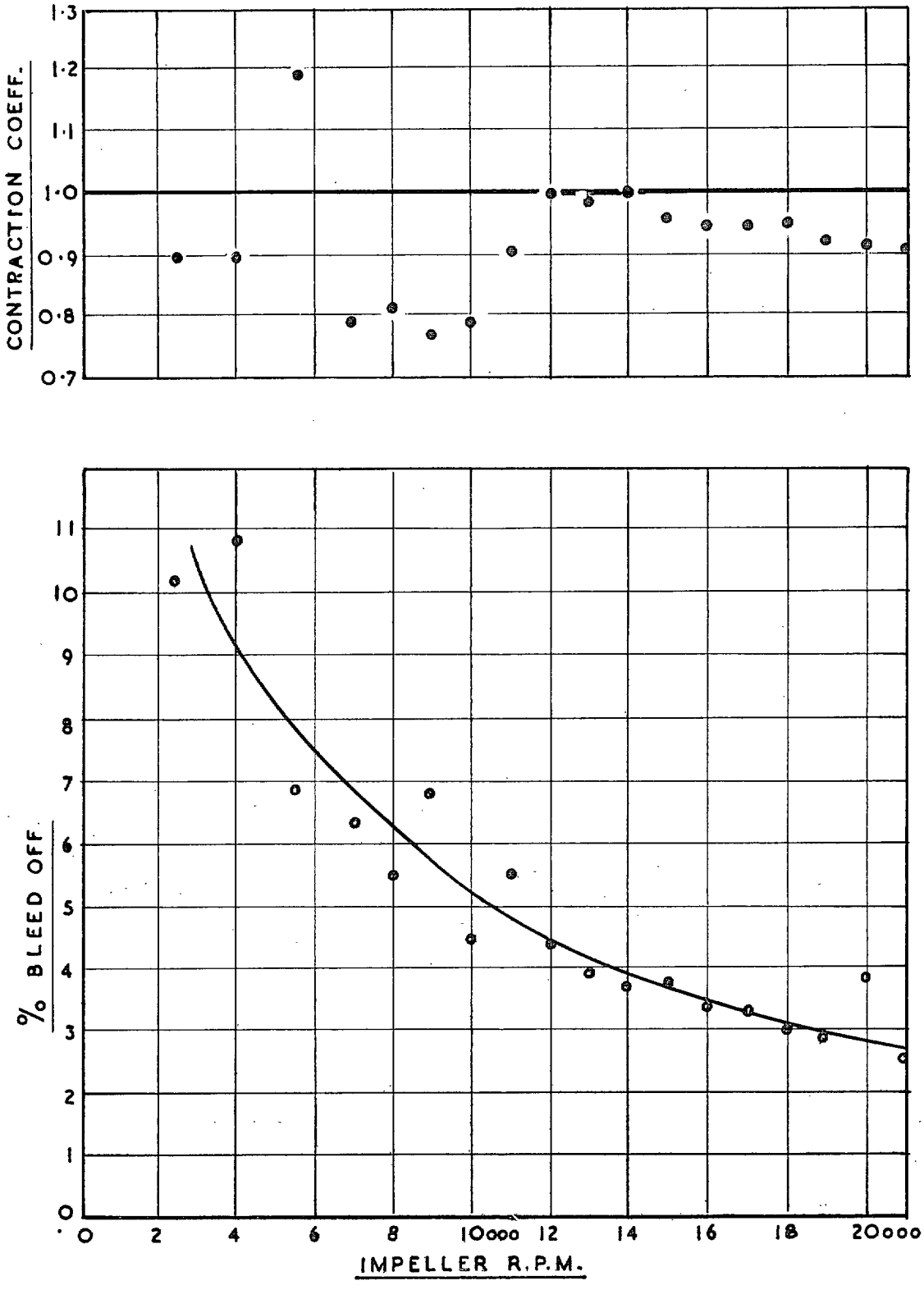

FIG. 7. Contraction and bleed-off conditions.

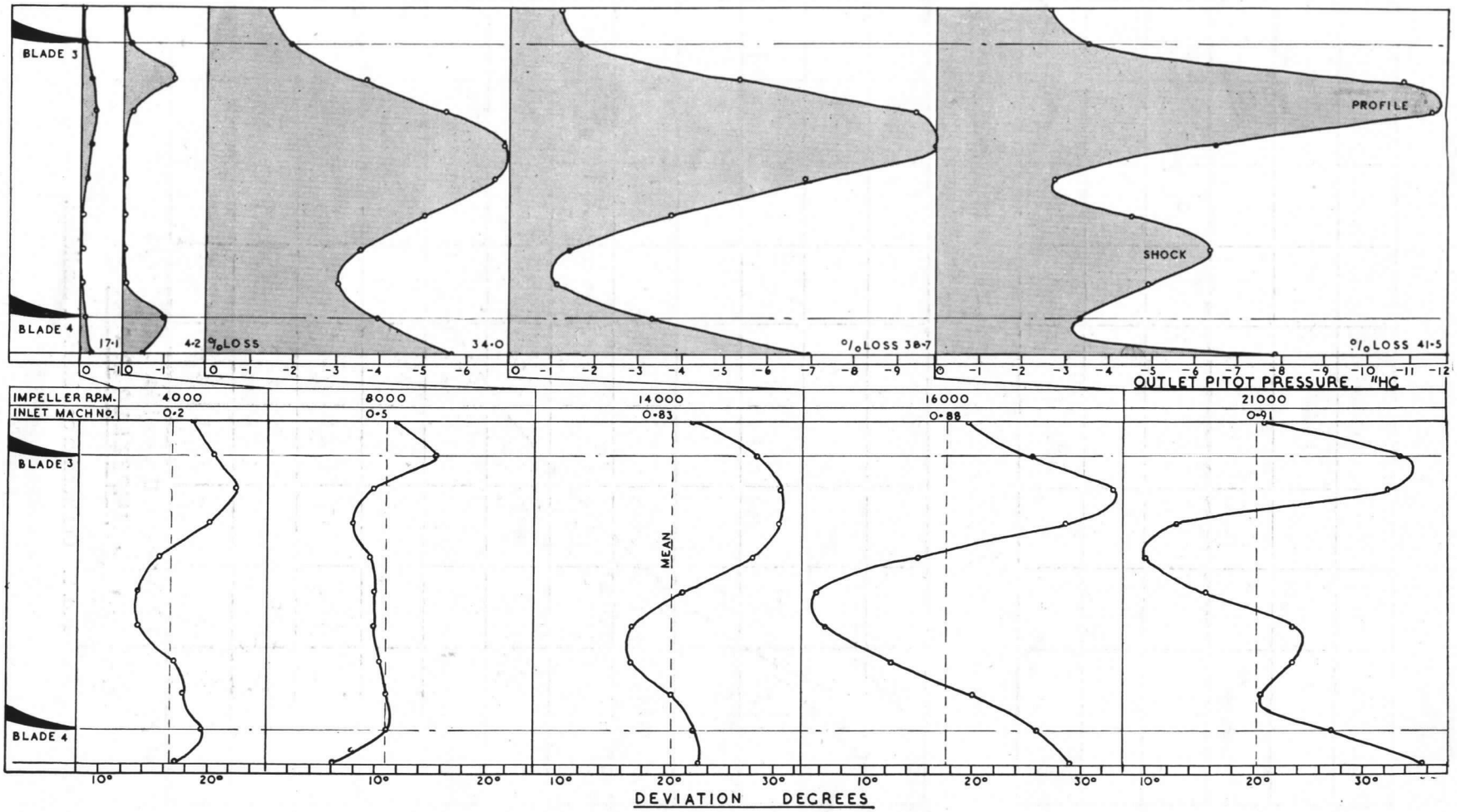

FIG. 8. Wake movements at mid-height of passage.

To face p. 20

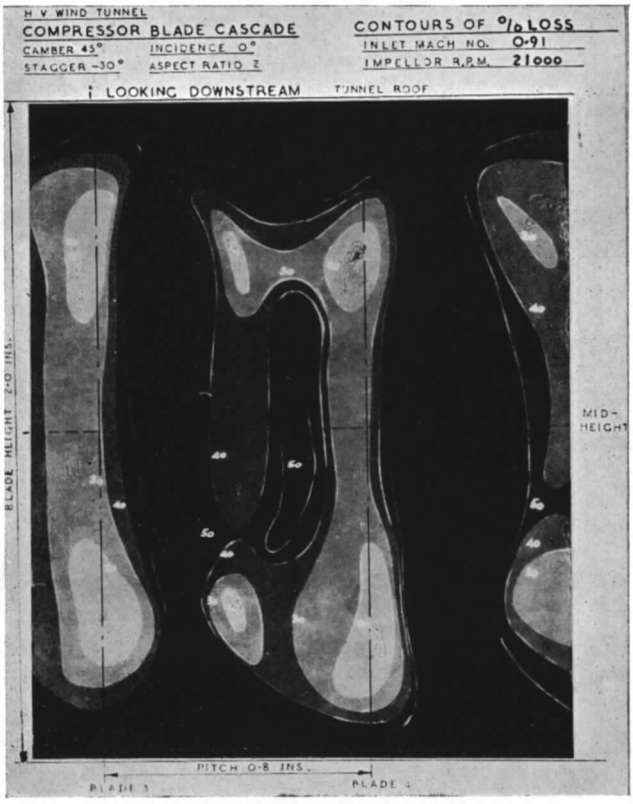

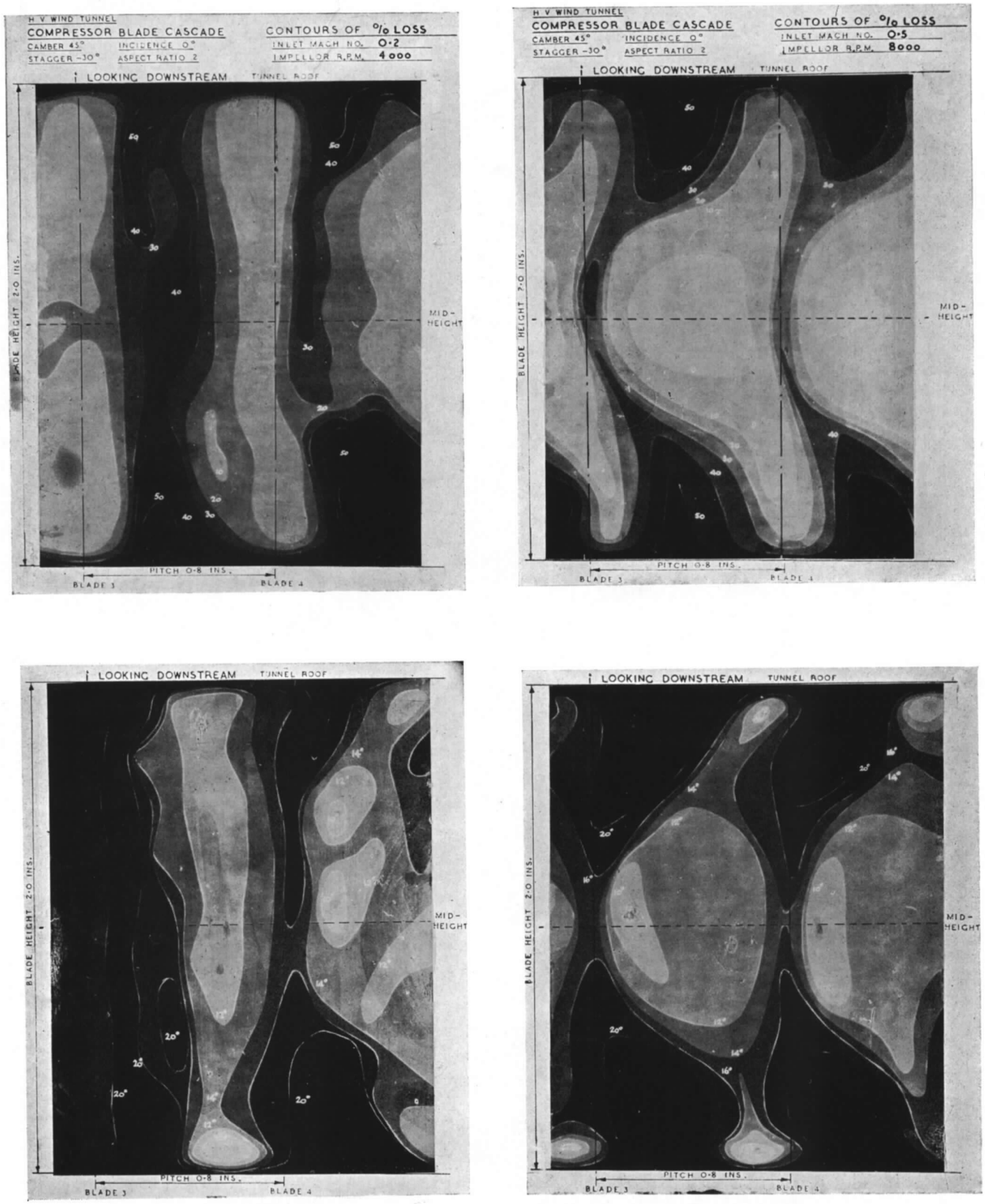

FIG. 9. Three-dimensional percentage loss and deviation contours.

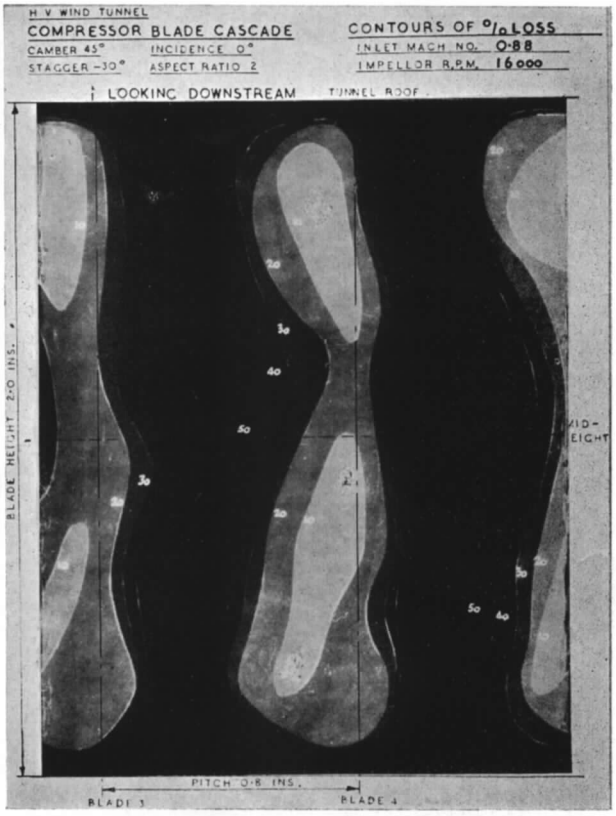

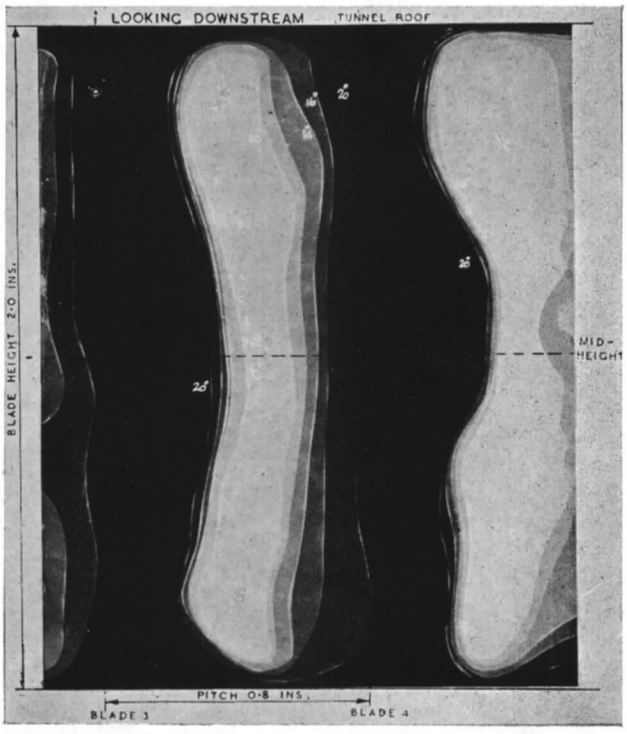

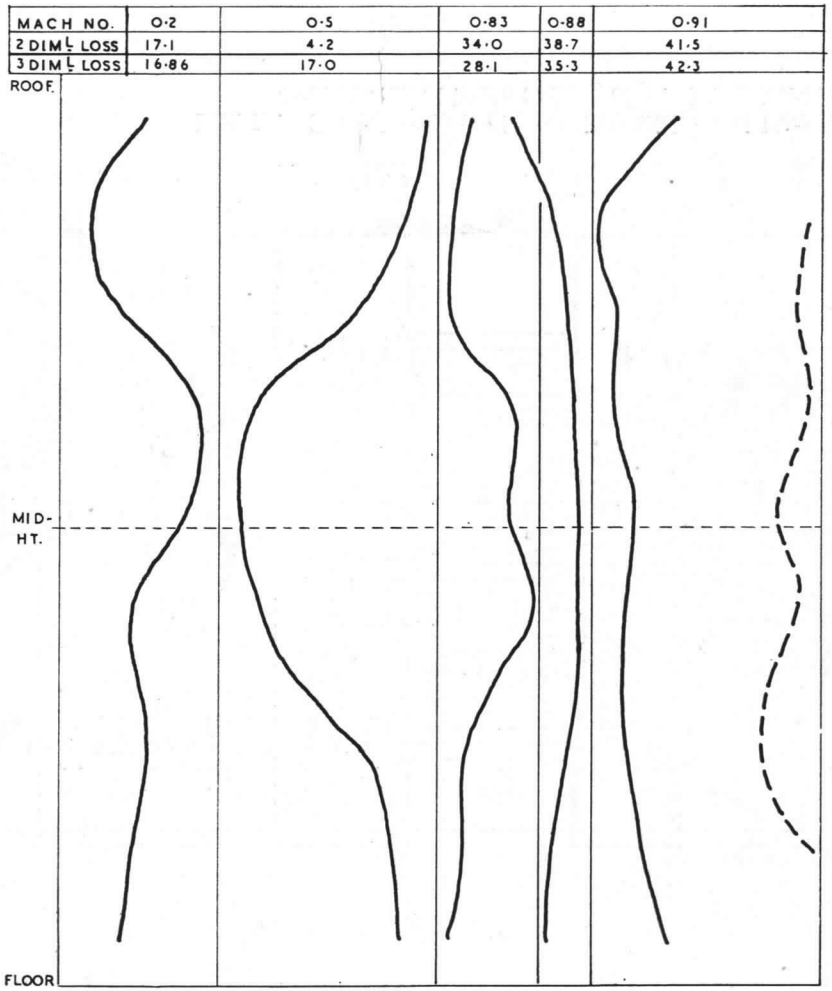

FIG. 10. Peak loss traces.

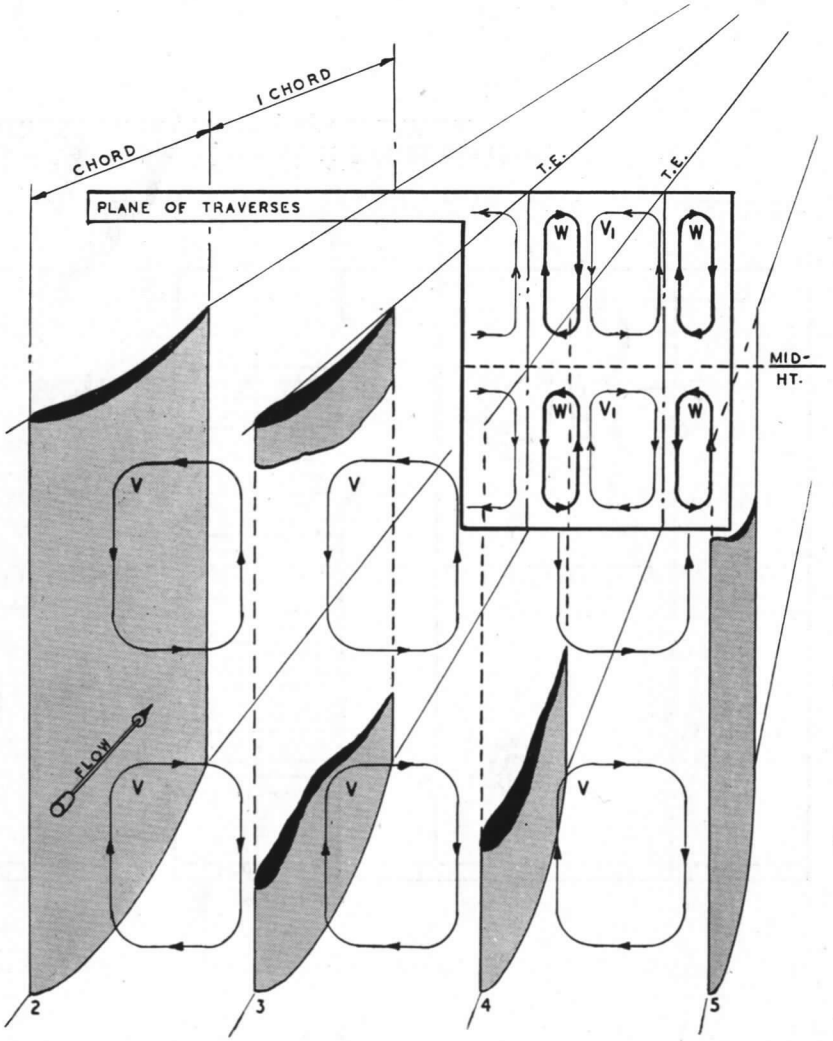

FIG. 11. Diagrammatic representation of secondary flow.

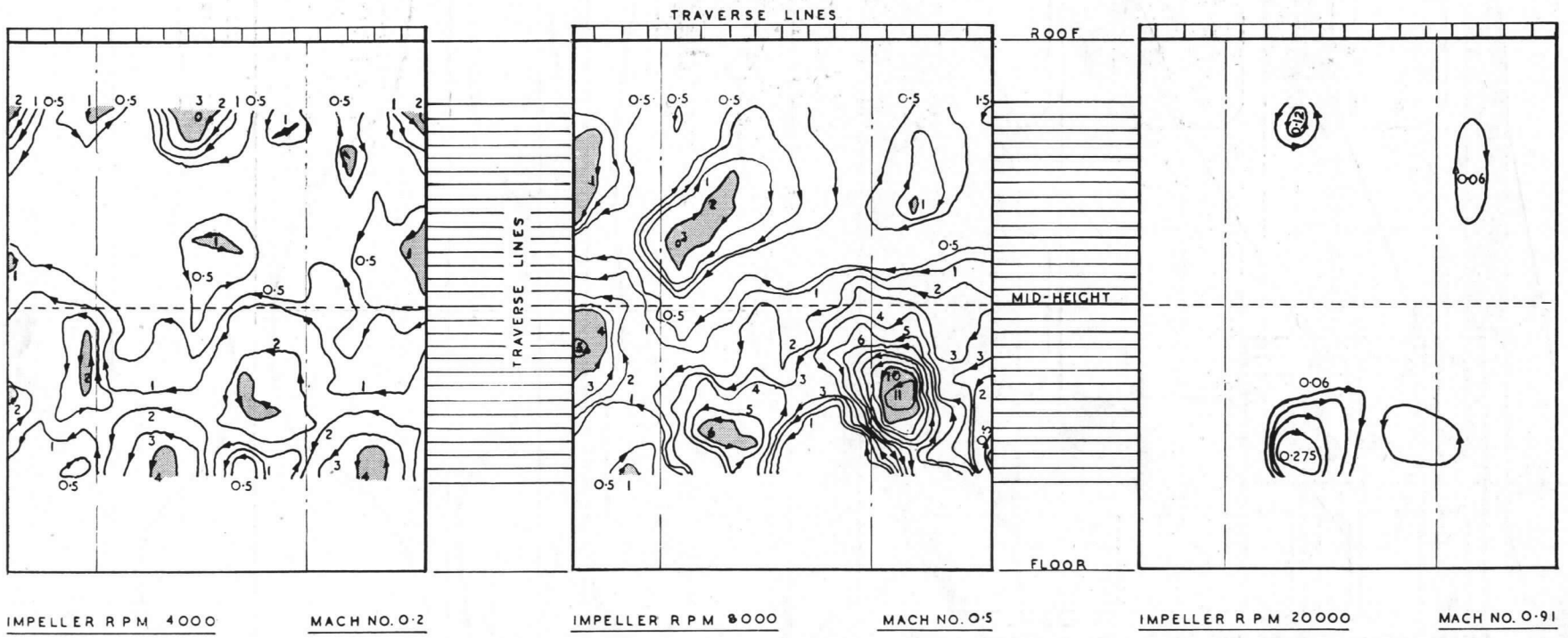

FIG. 12. Secondary-flow observations with a swirl vane. 150-speed contours in r.p.m. × 1000 at one chord downstream of blade trailing edge. Direction of rotation indicated when looking downstream.

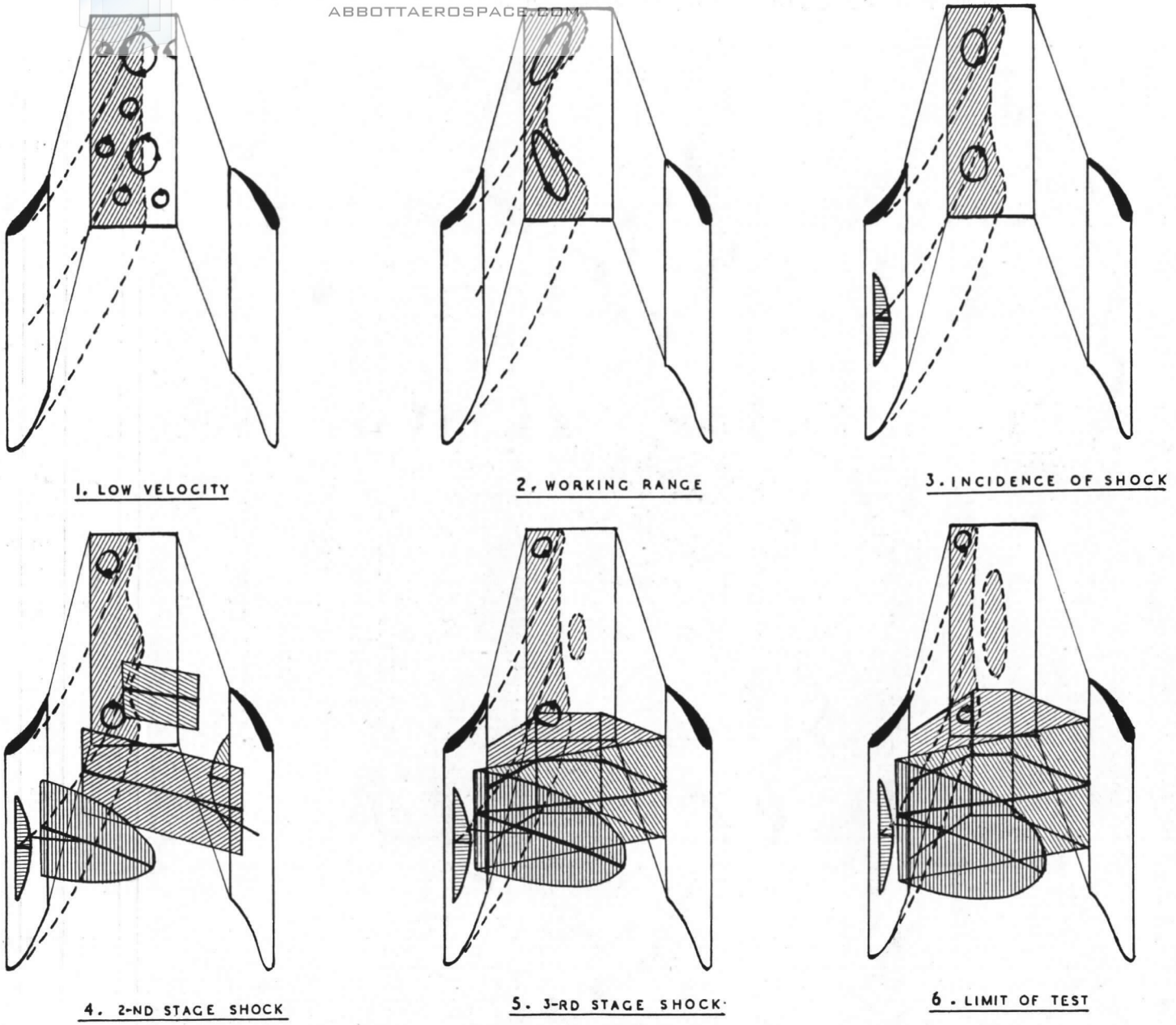

FIG. 13. Summary of flow characteristics.

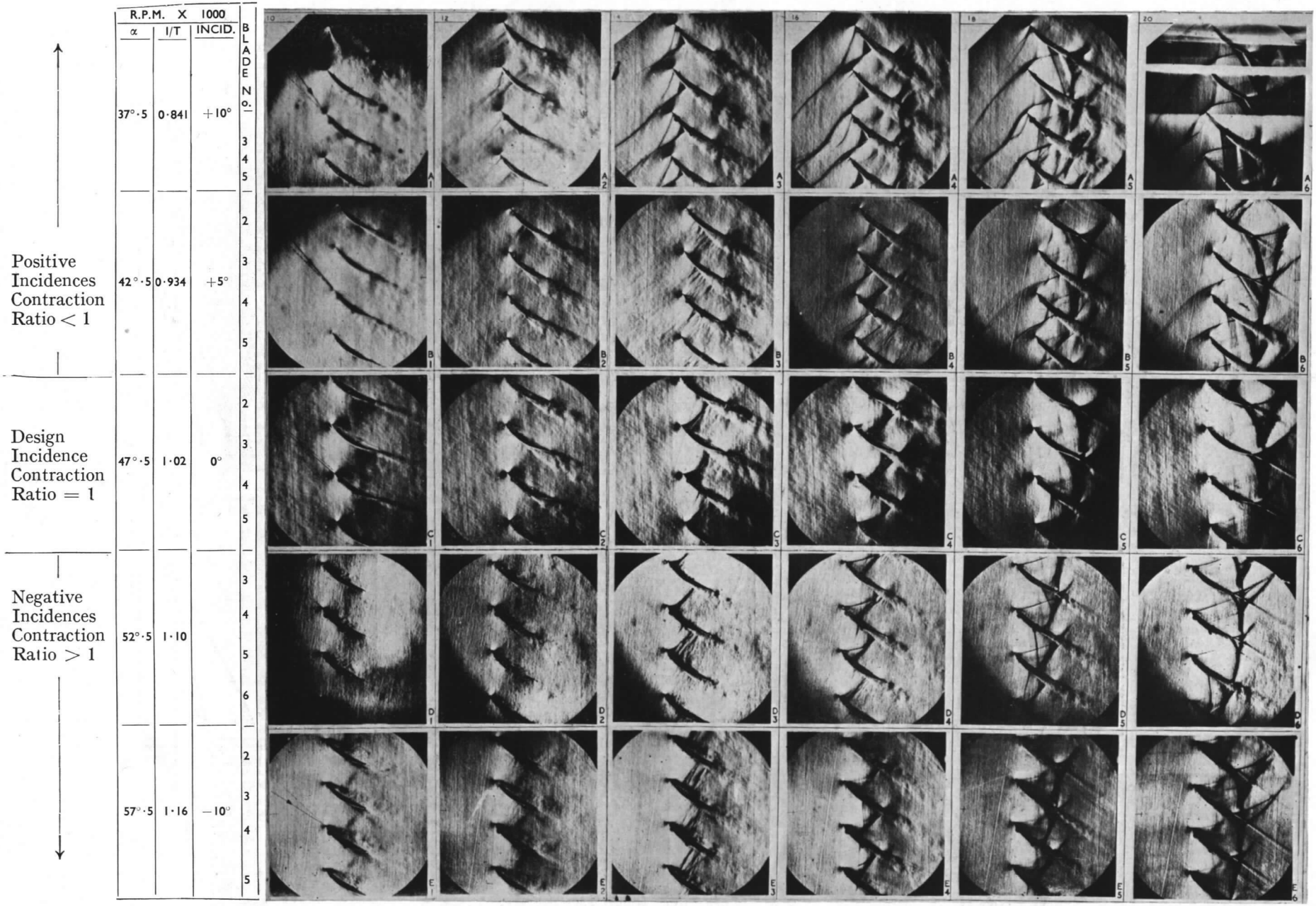

FIG. 14. Photographic summary of shock-wave development.

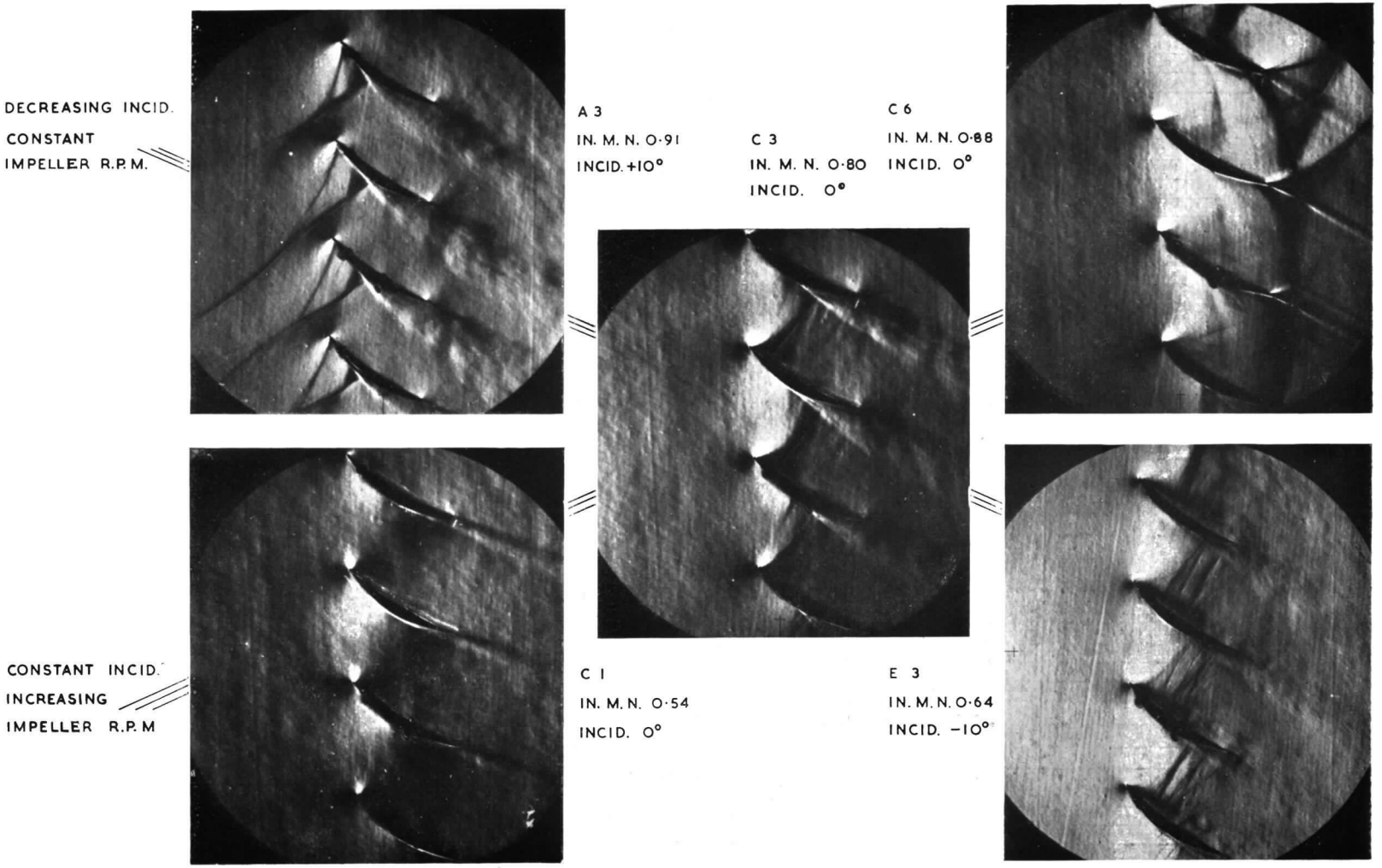

FIG. 15.

FIG. 16. TABULATION OF RESULTS

INCIDENCE & CONT. RATIO		UNIT	−10°								1·16		−5°									1·10
1	TEST NUMBER		412	411	410	410R	408	407	409	413	414	415	393	392	391	390	389	388	397	394	395	396
2	AMBIENT TEMP.	°C. AB	295	297	296	295	293	293	295	297	297	290	290	290	290	291	290	294	292	292	292	290
3	IMPELLER R.P.M.	X10³	4	6	8	8	10	12	14	16	18	20	4	6	8	10	12	14	15	16	18	20
	INLET																					
4	MACH NUMBER		0·18	0·28	0·39	0·39	0·48	0·56	0·64	0·66	0·67	0·67	0·18	0·30	0·42	0·52	0·62	0·70	0·74	0·75	0·76	0·77
5	VELOCITY	FT/SEC	196	315	431	430	525	612	685	707	718	714	198	338	455	565	660	747	785	788	804	808
6	REYNOLDS NUMBER	X10⁴	9·19	14·4	19·3	19·6	23·0	26·3	28·6	28·7	29·2	30·4	9·64	16·1	21·2	25·1	29·1	30·5	32·3	32·2	32·4	33·1
7	MASS FLOW	LB/SEC	0·94	1·47	1·98	1·98	2·26	2·54	2·76	2·77	2·82	2·87	0·92	1·52	1·96	2·31	2·60	2·73	2·85	2·84	2·85	2·88
	OUTLET																					
8	MACH NUMBER		0·14	0·25	0·37	0·39	0·46	0·56	0·68	0·75	0·85	0·93	0·20	0·28	0·40	0·49	0·59	0·68	0·76	0·80	0·89	0·96
9	VELOCITY	FT/SEC	155	285	403	433	500	609	731	803	890	960	218	306	439	529	638	724	800	844	925	990
10	DEVIATION	DEG.	2·8	0·5	0·8	1·5	0·7	−3·6	6·9	8·0	7·2	6·0	2·8	1·1	1·4	1·1	4·0	8·0	7·1	7·4	7·7	6·3
11	DEFLECTION	DEG.	14·7	17·0	16·7	16·0	16·8	13·9	10·6	9·5	10·3	11·5	19·7	21·4	21·1	21·4	18·5	14·6	15·4	15·1	14·8	16·2
12	TOTAL HEAD LOSS	%	6·06	4·71	6·13	5·10	4·99	8·92	13·58	22·80	26·70	34·80	6·40	3·43	2·50	2·53	7·07	16·02	13·22	15·55	22·30	30·0
13	PRESSURE RATIO		1·007	1·006	1·008	0·994	1·008	0·988	0·927	0·862	0·783	0·696	0·997	1·010	1·007	1·021	0·998	0·970	0·936	0·898	0·817	0·730
	BLEED - OFF																					
14	LEFT SIDEWALL	%	2·49	2·86	1·54	1·54	2·03	1·46	1·68	1·64	1·62	1·60	0·84	0·72	0·88	1·41	1·78	1·41	1·50	1·53	1·51	1·43
15	RIGHT SIDEWALL	%	0	0	0	0	0	0	0	0	0	0	0	0	0	0	0	0	0	0	0	0
16	ROOF	%	0	0	2·78	2·78	1·55	1·35	0·90	1·54	1·51	1·51	4·97	2·88	2·08	1·57	1·57	1·05	1·00	1·06	1·05	1·04
17	FLOOR	%	0	0	2·38	2·38	1·52	1·31	0·98	1·30	1·26	1·25	2·25	2·88	2·37	1·90	1·54	1·41	1·36	1·34	1·29	1·29
18	TOTAL	%	2·49	2·86	6·70	6·70	5·10	4·12	3·56	4·48	4·59	4·36	8·06	6·48	5·33	4·88	4·89	3·87	2·86	3·93	3·85	3·76
19	CONTRACTION COEFF.		1·021	0·962	0·935	0·877	0·918	0·910	0·905	0·911	0·892	0·896	0·752	0·904	0·853	0·862	0·877	0·924	0·970	0·881	0·766	0·900
20	OVERALL MACH NO.		0·135	0·271	0·383	0·408	0·475	0·585	0·720	0·821	0·922	1·02	0·196	0·278	0·405	0·492	0·620	0·735	0·804	0·855	0·960	1·05
	SPECIAL TESTS																					
	OPTICAL REF.NO.						E 1	E 2	E 3	E 4	E 5	E 6				D 1	D 2	D 3		D 4	D 5	D 6

INCIDENCE & CONT. RATIO		UNIT	0°												1·02	+ 5°									0·934	+10°								0·841
1	TEST NUMBER		368	366	367	365	364	373	363	374	362	375	370	376	369	371	384	383	382	380	378	387	379	381	385	386	402	401	400	399	398	403	404	405	406
2	AMBIENT TEMP.	°C AB	291	291	294	298	293	290	292	290	291	290	290	290	291	291	293	292	290	291	290	290	290	290	295	292	290	291	292	290	290	291	292	293	293
3	IMPELLOR R.P.M.	X10³	2·8	4	6	8	10	11	12	13	14	15	16	17	18	20	4	6	8	10	12	13	14	16	18	20	4	6	8	10	12	14	16	18	20
	INLET																																		
4	MACH NUMBER		0·10	0·17	0·31	0·42	0·54	0·61	0·71	0·72	0·80	0·85	0·87	0·87	0·87	0·88	0·20	0·34	0·46	0·59	0·75	0·82	0·89	0·94	0·98	0·99	0·22	0·34	0·48	0·62	0·76	0·91	0·99	1·00	1·03
5	VELOCITY	FT/SEC	105	190	345	466	591	652	756	760	842	886	908	908	905	919	217	369	496	630	794	857	926	965	1010	1008	246	389	522	662	806	942	1010	1036	1060
6	REYNOLDS NUMBER	X10⁴	5·07	9·08	15·9	20·3	25·8	28·2	31·4	31·9	33·7	35·0	35·3	35·0	34·8	35·2	10·2	17·3	22·6	27·5	33·1	34·3	36·3	35·9	36·4	36·1	11·7	17·8	22·9	28·2	32·2	35·5	36·4	36·9	38·4
7	MASS FLOW	LB/SEC	0·45	0·81	1·42	1·81	2·21	2·38	2·60	2·61	2·71	2·76	2·78	2·76	2·75	2·77	0·78	1·39	1·79	2·13	2·45	2·49	2·59	2·53	2·56	2·55	0·86	1·28	1·63	1·94	2·15	2·29	2·29	2·31	2·34
	OUTLET																																		
8	MACH NUMBER			0·13	0·28	0·39	0·48	0·53	0·61	0·61	0·66	0·72	0·76	0·80	0·83	0·89	0·15	0·29	0·39	0·51	0·62	0·66	0·71	0·77	0·87	0·92	0·15	0·28	0·34	0·40	0·53	0·64	0·73	0·83	0·96
9	VELOCITY	FT/SEC		147	309	437	525	569	660	658	708	763	803	836	868	924	168	315	423	554	666	705	752	809	907	956	164	305	375	440	576	689	776	873	992
10	DEVIATION	DEG.	6·7	4·3	2·6	2·7	3·2	2·6	1·2	1·6	5·0	6·4	6·9	7·0	7·0	8·0	4·9	4·5	4·7	5·5	6·5	5·1	6·3	8·0	8·6	6·6	5·7	6·6	6·1	6·1	7·8	9·2	9·5	8·0	6·4
11	DEFLECTION	DEG	20·8	23·2	24·9	24·8	24·3	24·9	26·3	25·9	22·5	21·2	20·6	20·5	20·5	19·5	27·6	28·0	27·8	27·0	26·0	27·4	26·3	24·5	23·9	25·9	31·9	30·9	31·4	31·4	29·7	28·3	28·0	29·5	31·2
12	TOTAL HEAD LOSS	%	11·83	7·05	2·97	2·75	2·28	2·94	5·04	5·37	13·54	13·52	15·40	18·05	18·95	23·20	5·45	5·28	3·92	5·84	5·46	6·80	10·80	19·60	23·0	27·80	20·3	13·67	16·35	19·46	21·70	25·30	33·20	32·80	33·50
13	PRESSURE RATIO			1·003	1·011	1·009	1·042	1·052	1·064	1·073	1·078	1·064	1·033	0·995	0·952	0·892	1·008	1·018	1·037	1·042	1·092	1·124	1·132	1·086	1·00	0·918	1·00	1·021	1·060	1·101	1·121	1·132	1·071	0·950	0·882
	BLEED - OFF																																		
14	LEFT SIDEWALL	%	4·62	1·77	1·31	1·71	1·42	1·07	0·93	1·19	1·38	1·30	1·28	1·29	1·17	1·10	0·62	0·36	0·28	0·60	0·79	1·04	1·26	1·07	1·16	0·90	5·78	4·15	3·52	3·50	0·24	1·38	1·15	1·06	0·98
15	RIGHT SIDEWALL	%	1·95	1·06	0·61	1·67	1·36	0	0	0	0	0	0	0	0	0	0·40	0	0	0	0	0	0	0	0	0	0	0	0	0	0	1·36	0	0	0
16	ROOF	%	1·20	1·83	1·51	1·76	1·42	1·47	1·56	1·41	1·31	1·32	1·30	1·31	1·14	1·19	3·05	2·98	2·74	2·02	1·46	1·38	1·27	1·19	1·18	1·15	5·12	3·26	2·83	2·12	1·69	1·42	1·42	1·39	1·37
17	FLOOR	%	1·92	1·50	1·49	1·88	1·45	1·59	1·19	1·09	1·06	1·04	1·04	1·05	1·08	1·05	3·01	2·91	2·36	1·77	1·15	1·19	1·08	0·97	0·91	0·94	4·10	3·06	3·05	2·31	1·82	1·40	1·33	1·30	1·28
18	TOTAL	%	9·69	6·16	4·92	7·02	5·65	4·13	3·68	3·69	3·75	3·66	3·62	3·65	3·39	3·34	7·08	6·25	5·38	4·39	3·40	3·61	3·61	3·23	3·25	2·99	15·00	10·47	9·40	7·93	3·76	5·56	3·90	2·75	3·63
19	CONTRACTION COEFF			1·010	0·856	0·818	0·861	0·855	0·850	0·850	1·012	1·058	1·050	1·038	1·028	1·038	0·924	0·835	0·820	0·800	0·822	0·830	0·855	0·858	0·862	0·855	0·978	0·825	0·877	0·930	0·886	0·892	0·884	0·880	0·825
20	OVERALL MACH NO.			0·141	0·281	0·401	0·485	0·535	0·635	0·636	0·720	0·782	0·835	0·876	0·915	0·988	0·160	0·290	0·392	0·526	0·645	0·690	0·762	0·870	0·983	1·05	0·180	0·302	0·390	0·480	0·635	0·797	0·923	1·02	1·07
	SPECIAL TESTS																																		
	OPTICAL REF.NO						C 1		C 2		C 3		C 4		C 5	C 6				B 1	B 2		B 3	B 4	B 5	B 6				A 1	A 2	A 3	A 4	A 5	A 6

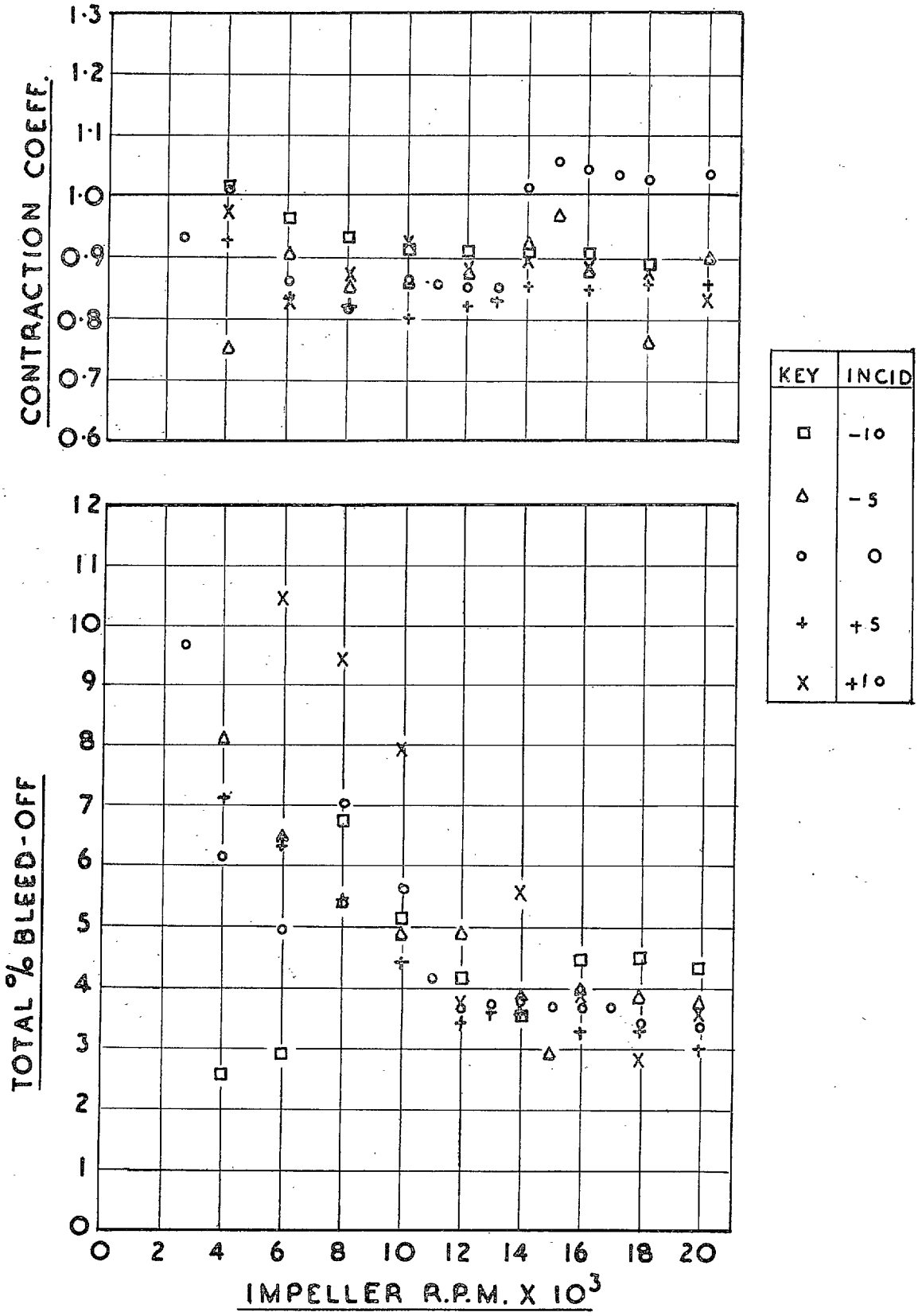

FIG. 17. Contraction coefficients and bleed-off qualities.

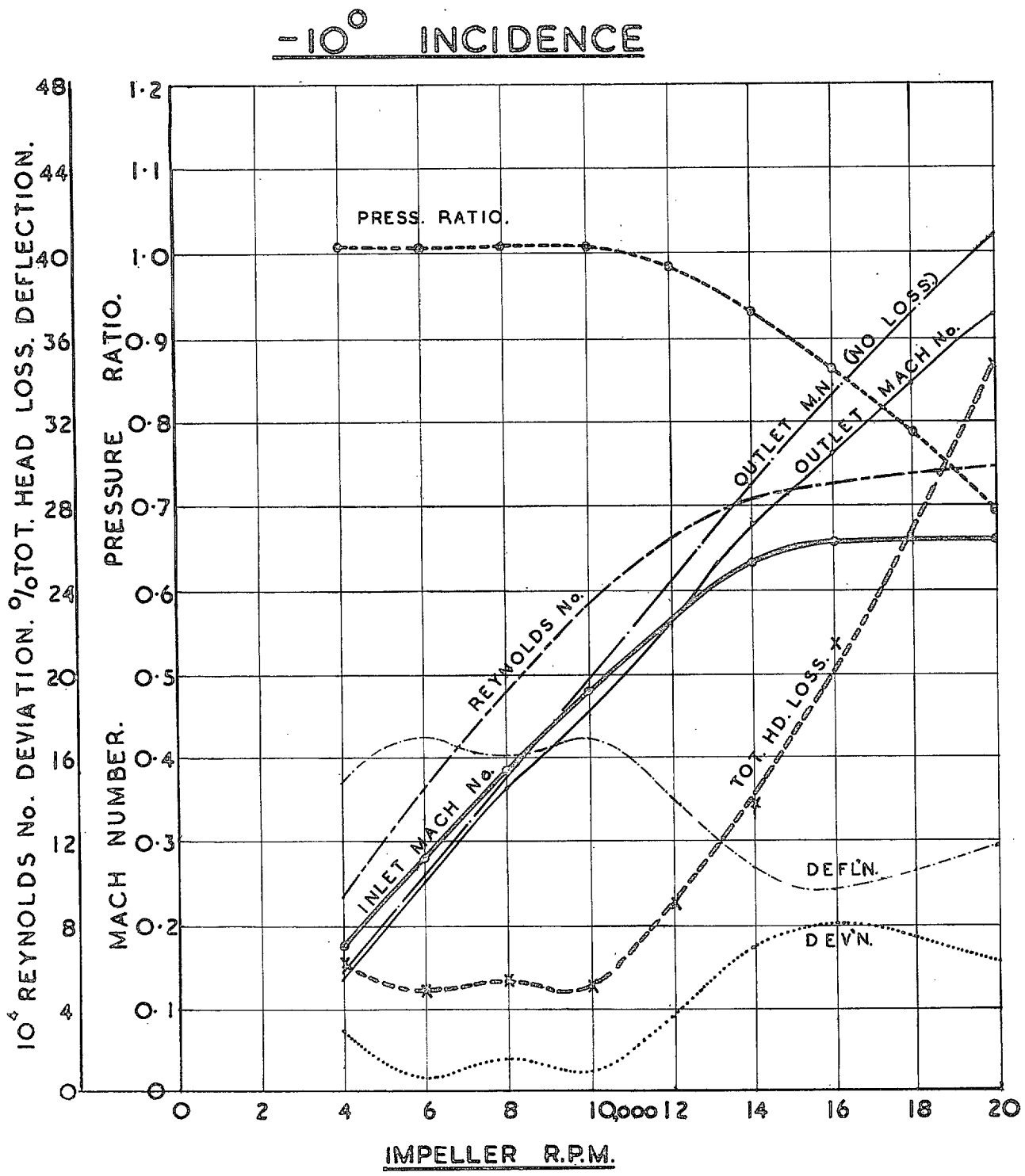

FIG. 18—1. Performance characteristics.

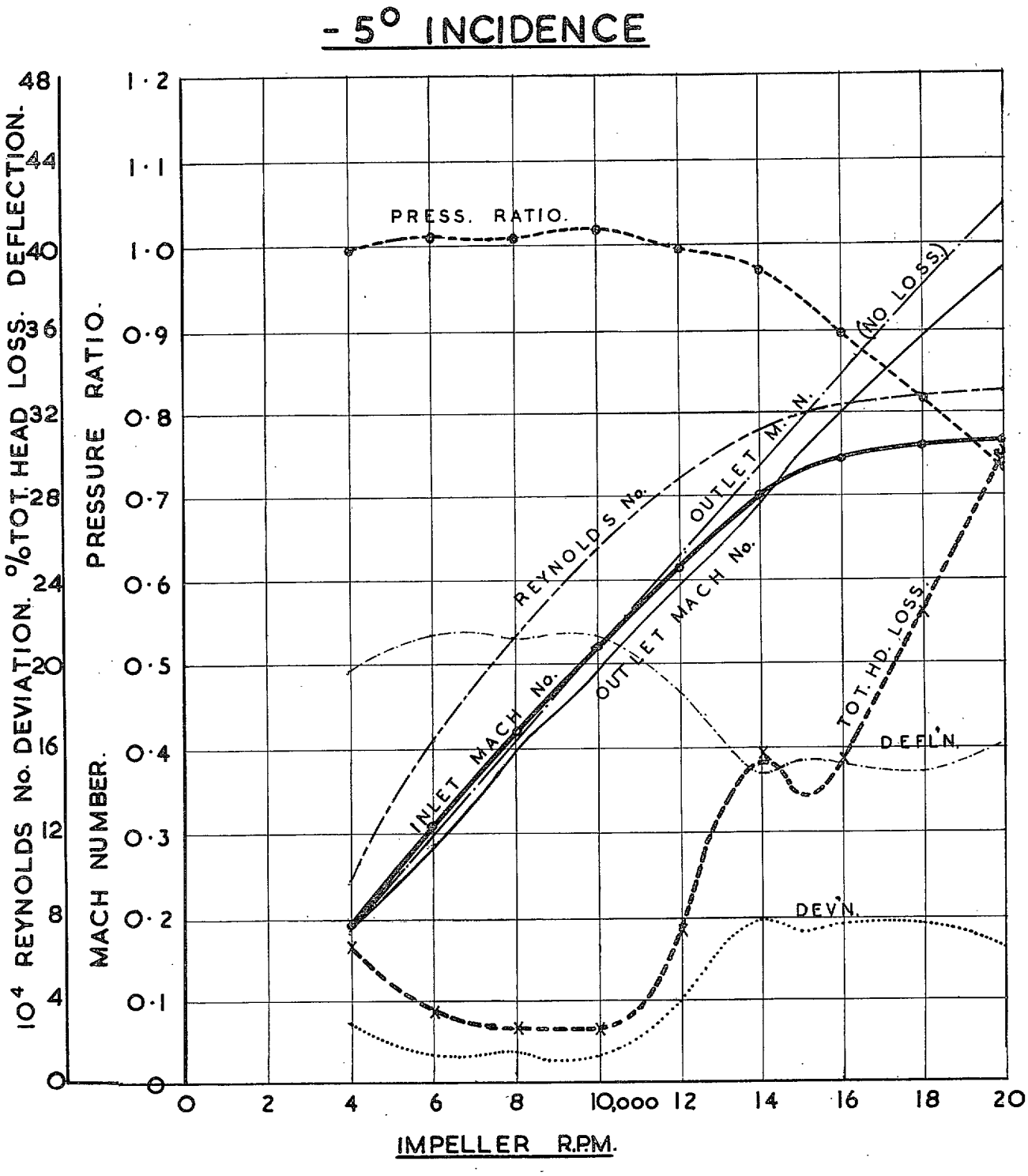

FIG. 18—2.

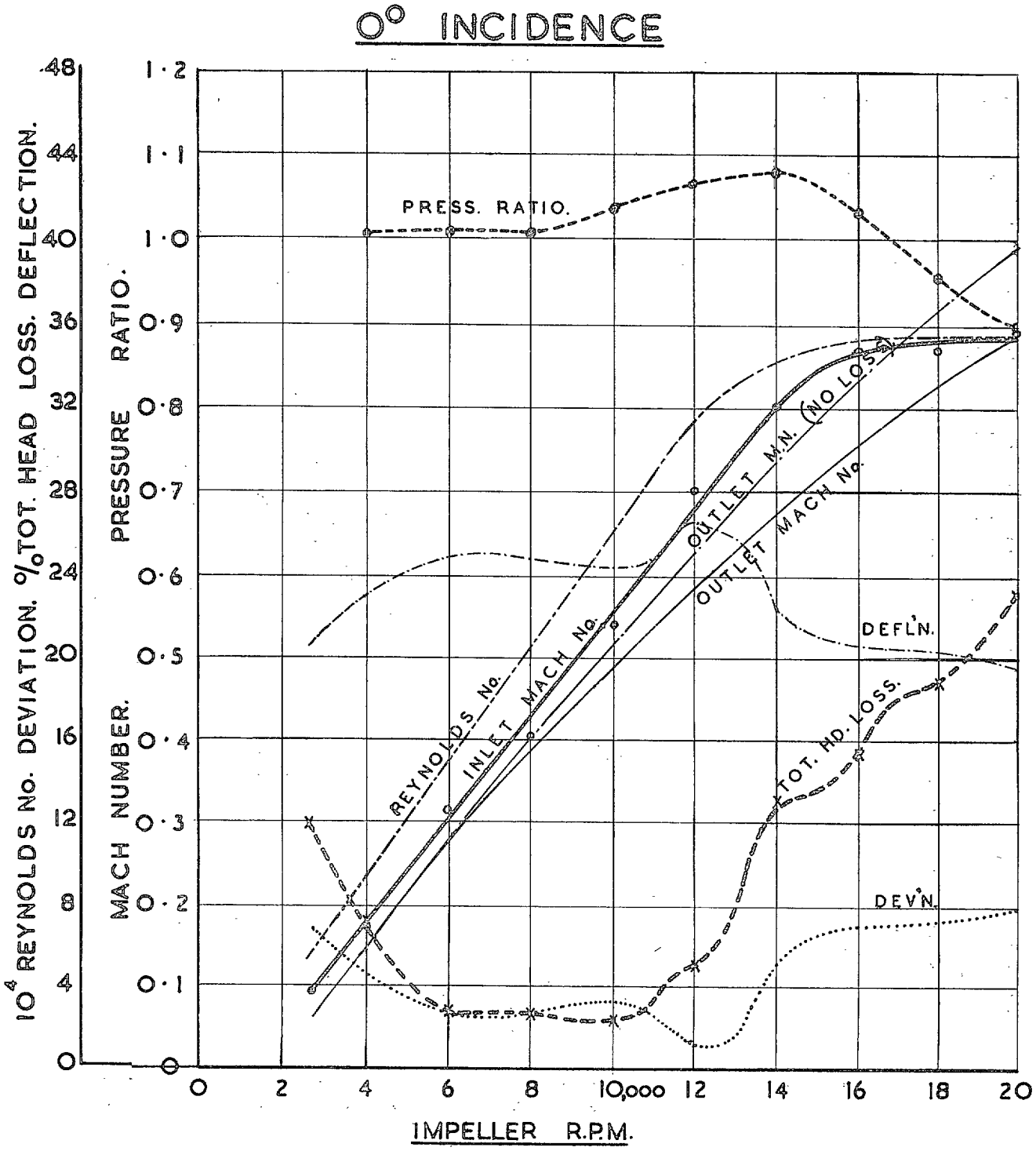

FIG. 18—3.

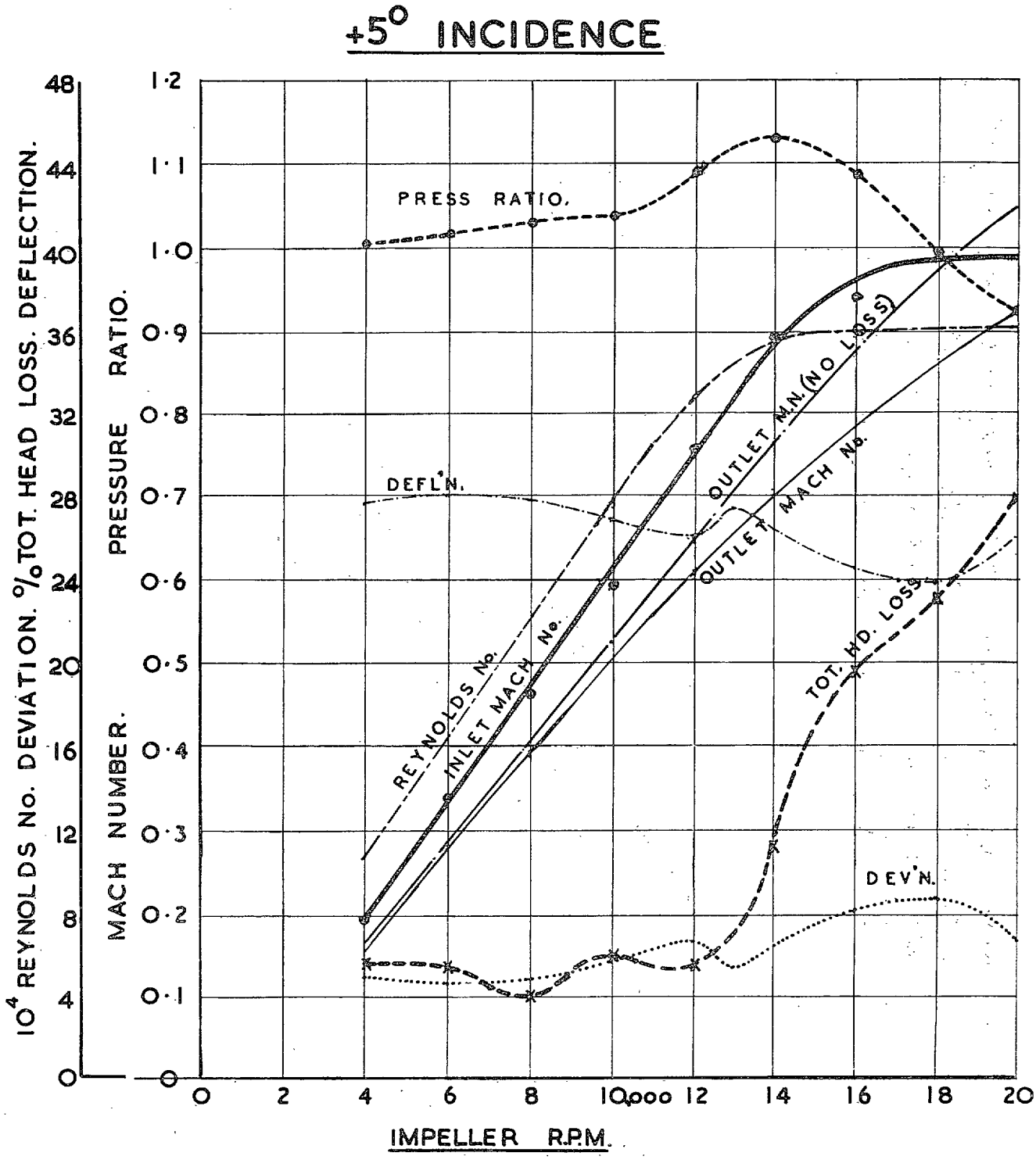

FIG. 18—4.

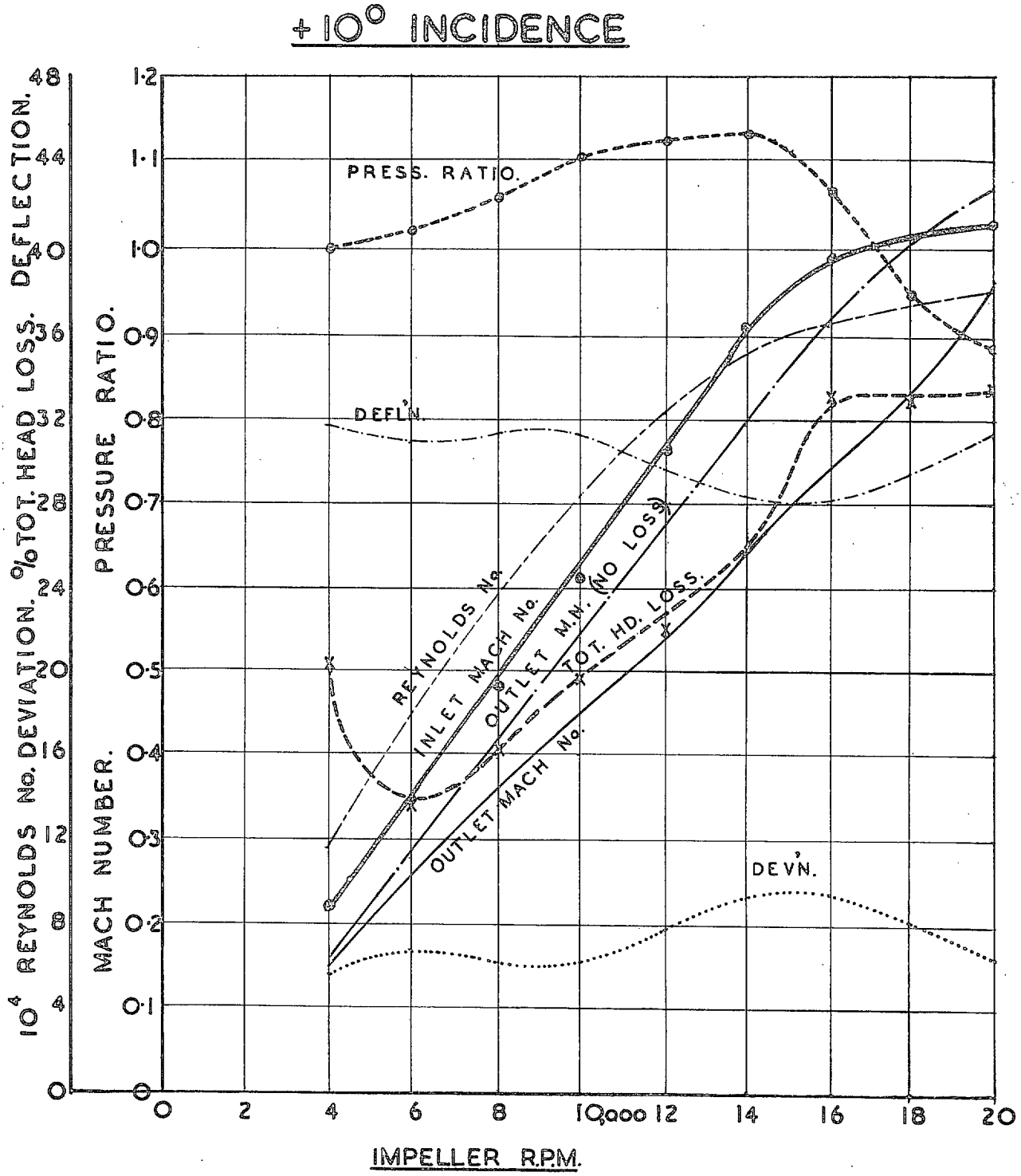

FIG. 18—5.

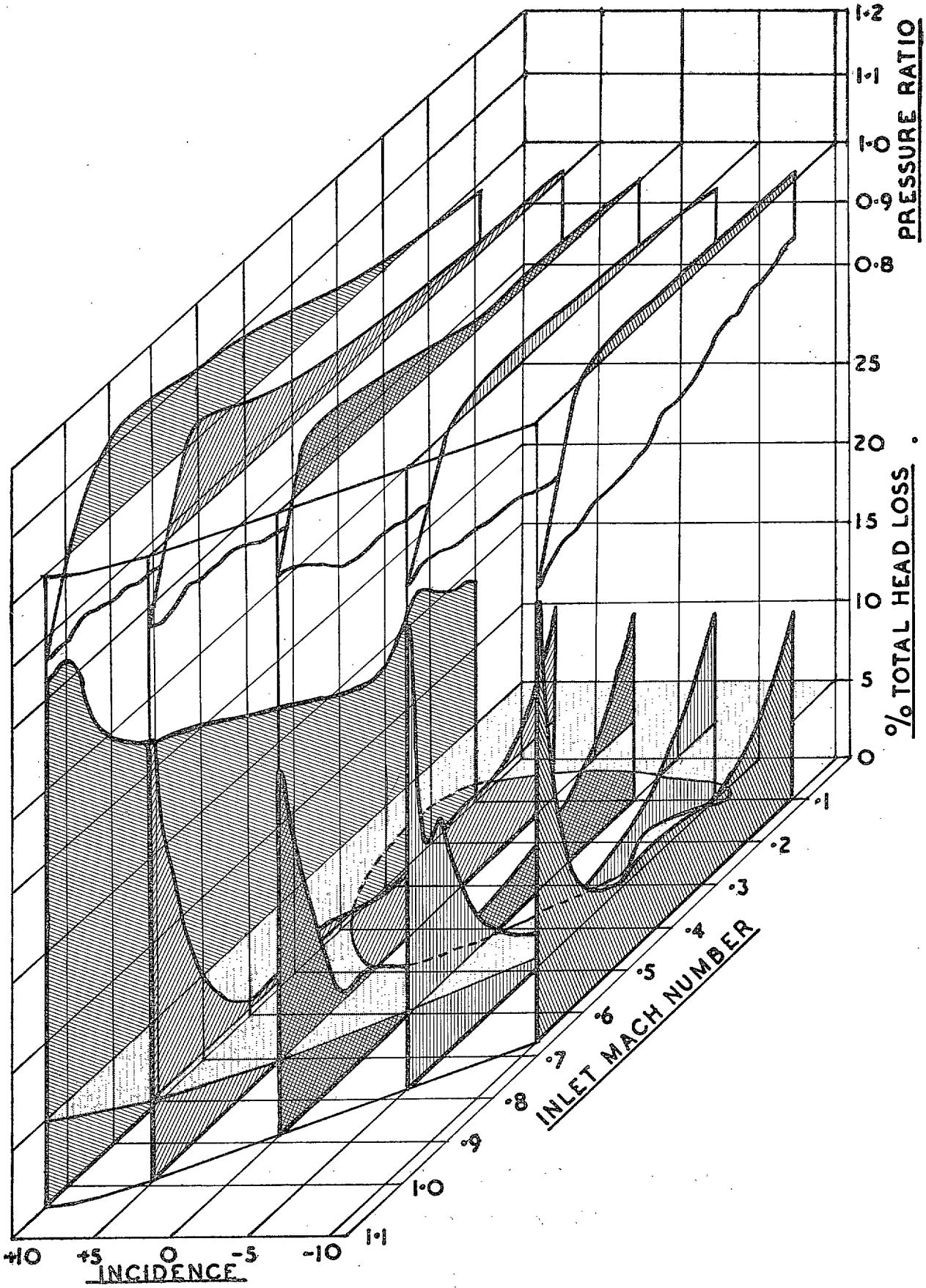

FIG. 19. Three-dimensional graph.

SIGNIFICANT DETAILS.	PART 2	PART 1
LEADING EDGE	SHARP	BLUNT: RAF 27+10%
CAMBER	27·5°	45°
CONTRACTION RATIO	1·02	0·916
MAX THICKNESS AT % CH.	50	32·6

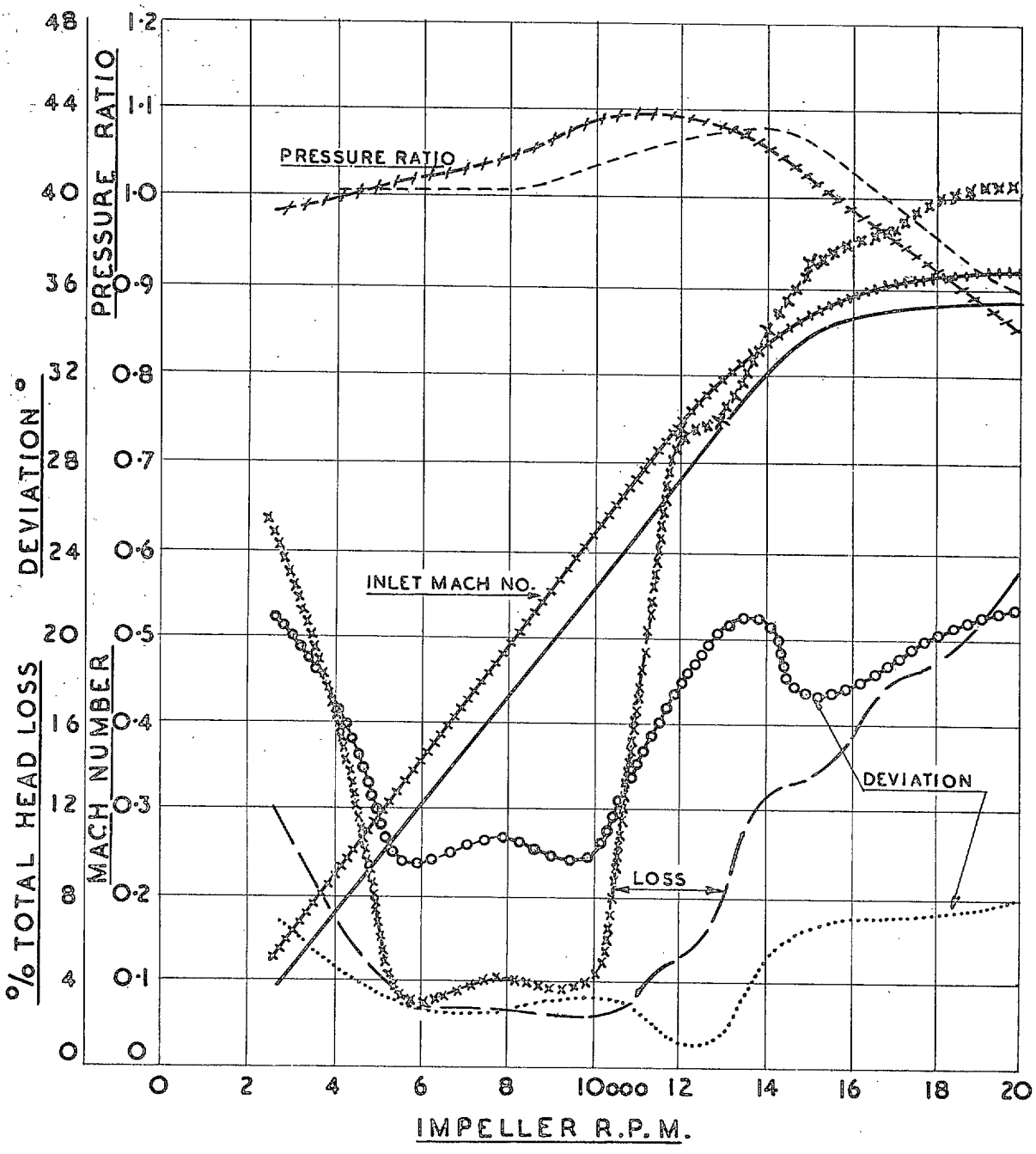

FIG. 20. Comparison of characteristics at 0 deg incidence.

NOTE: The accentuated curves refer to Part 1.

(60593) Wt. 17/680 K.9 4/54 Hw.

PRINTED IN GREAT BRITAIN

Publications of the Aeronautical Research Council

ANNUAL TECHNICAL REPORTS OF THE AERONAUTICAL RESEARCH COUNCIL (BOUND VOLUMES)

1936 Vol. I. Aerodynamics General, Performance, Airscrews, Flutter and Spinning. 40*s*. (40*s*. 9*d*.)
Vol. II. Stability and Control, Structures, Seaplanes, Engines, etc. 50*s*. (50*s*. 10*d*.)

1937 Vol. I. Aerodynamics General, Performance, Airscrews, Flutter and Spinning. 40*s*. (40*s*. 10*d*.)
Vol. II. Stability and Control, Structures, Seaplanes, Engines, etc. 60*s*. (61*s*.)

1938 Vol. I. Aerodynamics General, Performance, Airscrews. 50*s*. (51*s*.)
Vol. II. Stability and Control, Flutter, Structures, Seaplanes, Wind Tunnels, Materials. 30*s*. (30*s*. 9*d*.)

1939 Vol. I. Aerodynamics General, Performance, Airscrews, Engines. 50*s*. (50*s*. 11*d*.)
Vol. II. Stability and Control, Flutter and Vibration, Instruments, Structures, Seaplanes, etc. 63*s*. (64*s*. 2*d*.)

1940 Aero and Hydrodynamics, Aerofoils, Airscrews, Engines, Flutter, Icing, Stability and Control, Structures, and a miscellaneous section. 50*s*. (51*s*.)

1941 Aero and Hydrodynamics, Aerofoils, Airscrews, Engines, Flutter, Stability and Control, Structures. 63*s*. (64*s*. 2*d*.)

1942 Vol. I. Aero and Hydrodynamics, Aerofoils, Airscrews, Engines. 75*s*. (76*s*. 3*d*.)
Vol. II. Noise, Parachutes, Stability and Control, Structures, Vibration, Wind Tunnels. 47*s*. 6*d*. (48*s*. 5*d*.)

1943 Vol. I. (*In the press.*)
Vol. II. (*In the press.*)

ANNUAL REPORTS OF THE AERONAUTICAL RESEARCH COUNCIL—

1933–34	1*s*. 6*d*. (1*s*. 8*d*.)	1937	2*s*. (2*s*. 2*d*.)
1934–35	1*s*. 6*d*. (1*s*. 8*d*.)	1938	1*s*. 6*d*. (1*s*. 8*d*.)
April 1, 1935 to Dec. 31, 1936.	4*s*. (4*s*. 4*d*.)	1939–48	3*s*. (3*s*. 2*d*.)

INDEX TO ALL REPORTS AND MEMORANDA PUBLISHED IN THE ANNUAL TECHNICAL REPORTS, AND SEPARATELY—

April, 1950 - - - - R. & M. No. 2600. 2*s*. 6*d*. (2*s*. 7½*d*.)

AUTHOR INDEX TO ALL REPORTS AND MEMORANDA OF THE AERONAUTICAL RESEARCH COUNCIL—

1909–1949. R. & M. No. 2570. 15*s*. (15*s*. 3*d*.)

INDEXES TO THE TECHNICAL REPORTS OF THE AERONAUTICAL RESEARCH COUNCIL—

December 1, 1936 — June 30, 1939.	R. & M. No. 1850.	1*s*. 3*d*. (1*s*. 4½*d*.)
July 1, 1939 — June 30, 1945.	R. & M. No. 1950.	1*s*. (1*s*. 1½*d*.)
July 1, 1945 — June 30, 1946.	R. & M. No. 2050.	1*s*. (1*s*. 1½*d*.)
July 1, 1946 — December 31, 1946.	R. & M. No. 2150.	1*s*. 3*d*. (1*s*. 4½*d*.)
January 1, 1947 — June 30, 1947.	R. & M. No. 2250.	1*s*. 3*d*. (1*s*. 4½*d*.)
July, 1951.	R. & M. No. 2350.	1*s*. 9*d*. (1*s*. 10½*d*.)

Prices in brackets include postage.

Obtainable from

HER MAJESTY'S STATIONERY OFFICE

York House, Kingsway, London, W.C.2; 423 Oxford Street, London, W.1 (Post Orders: P.O. Box 569, London, S.E.1); 13a Castle Street, Edinburgh 2; 39, King Street, Manchester, 2; 2 Edmund Street, Birmingham 3; 1 St. Andrew's Crescent, Cardiff; Tower Lane, Bristol 1; 80 Chichester Street, Belfast, or through any bookseller

S.O. Code No. 23-2792